

# THE INFRARED LIMIT OF THE QCD DIRAC SPECTRUM AND APPLICATIONS OF CHIRAL RANDOM MATRIX THEORY TO QCD

J.J.M. Verbaarschot

*Department of Physics and Astronomy, SUNY Stony Brook,  
Stony Brook, NY 11790, USA,*

*e-mail: verbaarschot@nuclear.physics.sunysb.edu*

In the first part of these lectures we discuss the infrared limit of the spectrum of the QCD Dirac operator. We discuss the global symmetries of the QCD partition function and show that the Dirac spectrum near zero virtuality is determined by the pattern of spontaneous chiral symmetry breaking of a QCD-like partition function with additional bosonic valence quarks and their super-symmetric partners. We show the existence of an energy scale below which the fluctuations of the QCD Dirac spectrum are given by a chiral Random Matrix Theory (chRMT) with the global symmetries of the QCD partition function. Physically, for valence quark masses below this scale the partition function is dominated by the zero momentum modes. In the theory of disordered systems, this energy scale is known as the Thouless energy. In the second part of these lectures we discuss chRMT as a schematic model for the QCD partition function at nonzero temperature and chemical potential. We discuss novel features resulting from the non-Hermiticity of the Dirac operator. The analysis by Stephanov of the failure of the quenched approximation, the properties of Yang-Lee zeros, as well as the phase diagram of the chRMT partition function are discussed. We argue that a localization transition does not occur in the presence of light quarks. Several results will be derived in full detail. We mention the flavor symmetries of the QCD Dirac operator for two colors, the calculation of the valence quark mass dependence of the chiral condensate and the reduction of the chRMT partition function to the finite volume partition function.

## 1 Introduction

The two main phenomena that characterize the low-energy limit of QCD are confinement and chiral symmetry breaking. Because of confinement and the spontaneous breaking of chiral symmetry the low-lying states of QCD are given by the corresponding Goldstone bosons. At low temperatures we expect that the thermodynamics of the QCD partition function is that of a gas of (almost) massless pions. Mainly because of lattice simulations<sup>1,2,3,4</sup> we know that chiral symmetry is restored above a critical temperature of about 140 *MeV*. The order parameter of the chiral phase transition is the chiral condensate which through the Banks-Casher formula<sup>5</sup> is directly related to the spectral density of the QCD Dirac operator. This is our main motivation for detailed studies of QCD Dirac spectra.

One of the questions we wish to address in these lectures is to what extent the infrared limit of the Dirac spectrum can be obtained analytically. After all, the infrared limit of the QCD partition function is determined by the chiral Lagrangian describing Goldstone modes that become noninteracting at zero momenta. On the other hand we know from many studies of complex systems that the correlations of eigenvalues on the scale of the individual level spacings are universal and are given by Random Matrix Theory. More precisely, this has been formulated as the Bohigas-Giannoni-Schmit conjecture<sup>6</sup> which states that spectral correlations of a classically chaotic system are given by Random Matrix Theory (see Guhr et al.<sup>7</sup> for a comprehensive review).

The natural question one may ask is whether one can reconcile the universal nature of the chiral Lagrangian with the universal spectral correlations given by RMT. The first hint for the existence of a close connection came from the work of Leutwyler and Smilga<sup>8</sup> who found that the existence of a low-energy chiral Lagrangian imposes an infinite family of constraints on the spectrum of the Dirac operator. On the other hand, in the field of Random Matrix Theory it has been known for a long time that the spectral correlations can be described by a Goldstone manifold arising from the spontaneous breaking of symmetry between the advanced and retarded Greens functions<sup>9,10,11,12</sup>. The real breakthrough in this problem came with the introduction of valence quarks<sup>13,14,15,16,17</sup>. The idea is<sup>18</sup> to study a partition function that, in addition to the usual sea-quarks, contains a valence quark and its bosonic super-partner. After differentiation with respect to the source term and equating the fermionic and bosonic valence quark masses, the determinants with the valence quark masses cancel and we have access to the Dirac spectrum weighted by the standard QCD action. As is the case for the usual chiral Lagrangian, at low energies the partition function involving both sea quarks and valence quarks is completely determined by the scheme of chiral symmetry breaking and Lorentz-invariance and has been analyzed in the context of partially quenched chiral perturbation theory<sup>19,20</sup>. However, instead of constraints on QCD-Dirac spectra such as were obtained in the work by Leutwyler and Smilga<sup>8</sup>, we are now in a position to obtain an exact analytical expression for the Dirac spectrum in the domain of applicability of this so called partially quenched chiral perturbation theory.

As is the case for the usual chiral perturbation theory<sup>21</sup>, one can distinguish an important mass-scale. For sufficiently large volumes such that the contributions of the non-Goldstone modes are suppressed and valence quark masses

$$m_v \ll \frac{F^2}{\Sigma L^2} \quad (1)$$

(the pion decay constant is denoted by  $F$ ,  $\Sigma$  is the chiral condensate and  $L$

is the length of the box) the contribution of the nonzero momentum modes factorizes from the partition function and its mass dependence is given by the contribution from the zero momentum modes alone<sup>22,23,14,15,16,17</sup>. However, QCD is not the only theory with this zero momentum sector. Any theory with the same pattern of spontaneous symmetry breaking as QCD can be reduced to this zero momentum limit. In particular, chiral Random Matrix Theory<sup>24,25</sup>, with randomly distributed matrix elements of the Dirac operator is such a theory. In this case the strong interactions required to achieve a spontaneous breaking of chiral symmetry result from strongly non-local random interactions.

Such a picture is well-known from the theory of disordered mesoscopic systems (a number of recent reviews are available<sup>7,26,27</sup>). In this case, the scale below which Random Matrix Theory is valid is known as the Thouless energy, which is the inverse diffusion time of an electron through the sample<sup>28</sup>

$$E_c = \frac{\hbar D}{L^2}, \quad (2)$$

where  $D$  is the diffusion constant and  $L$  is the linear dimension of the box. The domain with  $\delta E \ll E_c$  is known as the ergodic domain whereas the domain  $E_c \ll \delta E \ll \hbar/\tau_e$  (with  $\tau_e$  is the elastic scattering time) is called the diffusive domain or the Altshuler-Shklovskii domain. In the case of QCD, the diffusion process is that of a quark propagating through the Yang-Mills fields in a 4+1 dimensional space time. The interpretation of spontaneous chiral symmetry breaking as a Mott transition was given earlier in<sup>29</sup>. By analogy with the Kubo formula,  $\Sigma$  plays the role of the conductivity<sup>29</sup>.

By now, this picture of the QCD gauge field configurations as a disordered system has been investigated in many lattice QCD simulations<sup>30,22,23,31,32,33,34,35,36,37,38,39,40,41,42,45,46,47,48</sup> and several instanton liquid simulations<sup>24,49,14,15</sup>. In particular, it has been confirmed that the scale below which chiral Random Matrix Theory is valid is given by the Thouless energy (1)<sup>14,15,34,42,48</sup>. It turns out that eigenvalue correlations are given by chRMT all the way up to this scale. Beyond this energy scale one has to take into account the contributions of the nonzero momentum modes. This can be done simply to one-loop order in chiral perturbation theory. In that way, one obtains analytical results for the valence quark mass dependence<sup>50,16</sup> of the chiral condensate in the Altshuler-Shklovskii domain.

In the first part of these lectures we will show that chRMT is an *exact* theory for the spectrum of the QCD Dirac operator in the ergodic domain. This is achieved by showing that in the range (1) the valence quark mass dependence of the chiral condensate obtained from the low-energy limit of the QCD

partition function coincides with the valence quark mass dependence obtained from chiral Random Matrix Theory. In the second part of these lectures we take a different route and use chRMT as a *schematic* model of the chiral phase transition<sup>51,52,53,54,55,57</sup>. In that case we obtain only *qualitative* results for the spectrum of the QCD Dirac operator and the chiral phase transition. For example, such models are the random matrix equivalent of a Landau-Ginzburg functional and give rise to mean field critical exponents. At the tricritical point where the upper critical dimension is three they provide us with a reliable description of the the infrared degrees of freedom<sup>58</sup>. The advantage of using random matrix models as opposed to a Landau-Ginzburg functional is that one has access to the Dirac spectrum. In particular, at nonzero chemical potential, this has provided us with valuable insights in the effects of non-Hermiticity on the properties of the QCD partition function<sup>54,59</sup>. The common ingredient of chRMT and QCD at nonzero chemical potential is that the phase of the fermion determinant due to the non-Hermiticity makes Monte Carlo simulations impossible. Since the chRMT partition function can be evaluated analytically, we are in a position to analyze some of these problems in great detail. In this way, a complete analytical understanding of the failure of the quenched approximation at nonzero chemical potential has been obtained<sup>54</sup>.

In the first lecture (section 2) we summarize the main properties of the Euclidean QCD partition function. We discuss in detail the global symmetries and give a brief review of lattice QCD (see lectures by Tom Blum<sup>60</sup> for more details). In the second lecture we analyze the infrared limit of the QCD partition function (section 3). We discuss the domain of validity of the zero momentum limit of the effective chiral partition function and introduce the partially quenched chiral partition function. An important point of this lecture is the discussion of the integration manifold. Explicit calculations of the valence quark mass dependence of the chiral condensate that rely on the structure of this Riemannian super-manifold are presented in section 4. Results are derived in detail both by perturbative and non-perturbative methods. In the third lecture we introduce chiral Random Matrix Theory. We discuss its main properties and emphasize the importance of universality (see section 5). In the second half of this lecture we present lattice QCD results for the statistical properties of Dirac eigenvalues and compare the results with random matrix theory. In the last lecture we introduce chiral Random Matrix Theory as a schematic model for the chiral phase transition. In the framework of this model, we discuss chiral symmetry breaking, quenching at nonzero chemical potential, Yang-Lee zeros in the complex chemical potential plane, the structure of Dirac spectra at nonzero chemical potential and the phase diagram

in the mass, chemical potential and temperature plane. Finally, we present general arguments that a localization transition does not occur in QCD with light quarks. Concluding remarks are made in section 8.

## 2 The QCD Partition Function

The QCD partition function describing strong interactions in a box of volume  $V_3 = L^3$  can be expressed in terms of the eigenvalues of the QCD Hamiltonian  $E_k$  as

$$Z^{QCD} = \sum_k e^{-\beta E_k}, \quad (3)$$

where  $\beta$  is the inverse temperature. At low temperatures ( $\beta \rightarrow \infty$ ) the partition function is dominated by the lightest states of the theory, namely the vacuum state, with an energy density of  $E_0/V_3$ , and massless excitations thereof. The partition function  $Z^{QCD}$  can be rewritten as Euclidean functional integral over the nonabelian gauge fields  $A_\mu$

$$Z^{QCD} = \int dA_\mu \prod_{f=1}^{N_f} \det(D + m_f) e^{-S_{YM}}, \quad (4)$$

where  $S_{YM}$  is the Yang-Mills action. We assume that this partition function is properly regularized, for example, by a lattice regularization. The gauge fields  $A_\mu$  are nonabelian gauge fields in Euclidean space time of volume  $V = L^3\beta$ . In terms of the generators,  $T_a$ , of  $SU(N_c)$  they can be written as

$$A_\mu = A_\mu^a \frac{T_a}{2}, \quad (5)$$

The anti-Hermitian Dirac operator is defined by

$$D = \gamma_\mu (\partial_\mu + iA_\mu), \quad (6)$$

where the  $\gamma_\mu$  are the Euclidean Dirac matrices with  $\{\gamma_\mu, \gamma_\nu\} = 2\delta_{\mu\nu}$ . In these lectures we will use the chiral representation of the gamma matrices (with diagonal  $\gamma_5$ ).

### 2.1 Symmetries of the QCD Partition Function

It is well-known that the QCD action is greatly constrained by gauge symmetry, Euclidean Poincaré invariance and renormalizability. These symmetries

determine the structure of the Dirac operator (6). In this section we will discuss the global symmetries of the Dirac operator. They play an essential role in its spectral properties in the deepest infrared. In particular, the chiral symmetry, the flavor symmetry and the anti-unitary symmetry of the continuum Dirac operator are discussed.

The chiral symmetry, or the  $U_A(1)$  symmetry, can be expressed in terms of the anti-commutation relation

$$\{\gamma_5, D\} = 0. \quad (7)$$

This implies that all nonzero eigenvalues occur in pairs  $\pm i\lambda_k$  with eigenfunctions given by  $\phi_k$  and  $\gamma_5\phi_k$ . If  $\lambda_k = 0$  the possibility exists that  $\gamma_5\phi_k \sim \phi_k$ , so that  $\lambda_k = 0$  is an unpaired eigenvalue. According to the Atiyah-Singer theorem, the total number of such zero eigenvalues is a topological invariant, i.e., it does not change under continuous transformations of the gauge field configuration. Indeed, this possibility is realized by the field of an instanton which is a solution of the classical equations of motion. On the other hand, it cannot be excluded that  $\lambda_k = 0$  while  $\phi_k$  and  $\gamma_5\phi_k$  are linearly independent. However, this imposes additional constraints on the gauge fields which will be violated by infinitesimal deformations. Generically, such situation does not occur.

In a decomposition according to the total number of topological zero modes, the QCD partition function can be written as

$$Z^{QCD} = \sum_{\nu} e^{i\nu\theta} Z_{\nu}^{QCD}, \quad (8)$$

where

$$Z_{\nu}^{QCD} = \langle \prod_f m_f^{\nu} \prod_k (\lambda_k^2 + m_f^2) \rangle_{\nu}. \quad (9)$$

Here,  $\langle \cdots \rangle_{\nu}$  denotes the average over gauge-field configurations with topological charge  $\nu$  weighted by the Yang-Mills action. In we introduce complex conjugated right-handed and left-handed masses we observe that the  $\theta$  dependence of the QCD partition function is only through the combination  $m e^{i\theta/N_f}$ .

A second important global symmetry is the flavor symmetry. This symmetry can be best explained by writing the fermion determinant in the QCD partition function as a functional integral over Grassmann variables,

$$\prod_f \det(D + m_f) = \int d\psi d\bar{\psi} e^{\int d^4x \sum_{f=1}^{N_f} \bar{\psi}^f (D + m_f) \psi^f}. \quad (10)$$

In a chiral basis with  $\psi_R = \gamma_5 \psi_L$  and  $\psi_L = -\gamma_5 \psi_R$ , this can be rewritten as

$$\prod_f \det(D + m_f) = \int d\psi d\bar{\psi} e^{\int d^4x [\sum_{f=1}^{N_f} \bar{\psi}_R^f D\psi_L^f + \bar{\psi}_L^f D\psi_R^f + \bar{\psi}_R^f m_f \psi_R^f + \bar{\psi}_L^f m_f \psi_L^f]}.$$
(11)

For  $m_f = 0$  we have the symmetry

$$\begin{aligned} \psi_L &\rightarrow U \psi_L, & \bar{\psi}_R &\rightarrow \bar{\psi}_R U^{-1}, \\ \bar{\psi}_L &\rightarrow \bar{\psi}_L V^{-1}, & \psi_R &\rightarrow V \psi_R. \end{aligned}$$
(12)

The only condition to be imposed on  $U$  and  $V$  is that their inverse exists. If the number of lefthanded modes is equal to the number of right-handed modes we thus have an invariance under  $Gl(N_f)_R \times Gl(N_f)_L$ . However, if the number of left-handed modes is not equal to the number of right-handed modes, the axial-symmetry group is broken to an  $Sl(N_f)$  subgroup whereas the vector symmetry with  $U = V$  remains unbroken. For  $m = 0$  the flavor symmetry is thus broken explicitly to  $Gl_V(N_f) \times Sl_A(N_f)$  by instantons or the anomaly.

What is much more important, though, is the spontaneous breaking of the axial flavor symmetry. From lattice QCD simulations and phenomenological arguments we know that the expectation value

$$\langle \bar{\psi}\psi \rangle = \langle \bar{\psi}_R \psi_R \rangle + \langle \bar{\psi}_L \psi_L \rangle \approx (240 \text{ MeV})^3$$
(13)

in the vacuum state of QCD instead of the symmetric possibility  $\langle \bar{\psi}\psi \rangle = 0$ . Phenomenologically, this is known because of the presence of Goldstone modes. The pions are much lighter than the  $\sigma$  mesons. The spontaneous breaking of the axial symmetry also follows from the absence of parity doublets. For example, the pion mass and the  $\delta$  (or  $a_0$ ) mass are very different ( $m_\pi = 135 \text{ MeV}$  and  $m_\delta = 980 \text{ MeV}$ ).

One easily verifies that  $\langle \bar{\psi}\psi \rangle$  is only invariant for  $U = V$ . The vacuum state thus breaks the chiral symmetry down to  $Gl_V(N_f)$ . Notice that only the axial symmetries are broken. This is in agreement with the Vafa-Witten theorem<sup>61</sup> which states that vector symmetries cannot be broken in vector-like theories such as QCD. We also observe that the *complete* axial group is broken. The reasons behind this maximum breaking<sup>62</sup> of chiral symmetry are less well understood. The Goldstone manifold is given by the maximum Riemannian submanifold of  $Sl_A(N_f)$  which is the usual manifold  $SU_A(N_f)$ . The complex extension of  $SU(N_f)$  does not give rise to additional conserved currents, and therefore, the total number of Goldstone modes remains the same (we thank J.C. Osborn for this remark).

For three or more colors the gauge fields are not related by complex conjugation and there are no anti-unitary symmetries. However, the situation is more interesting for  $N_c = 2$  which will be discussed in the next section.

## 2.2 Special Role of $N_c = 2$

The group  $SU(2)$  is the only nontrivial special unitary group that is pseudoreal. As will be shown in this section, the consequence is that for  $N_c = 2$  the symmetry group of the QCD partition function in the chiral limit is enlarged to  $U(2N_f)$ .

As before, the fermionic action is obtained by writing the determinant in the partition function as a Gaussian integral over the Grassmann fields  $\phi$  and  $\bar{\phi}$ . Using the chiral representation of the  $\gamma$  matrices with

$$\gamma_\mu = \begin{pmatrix} 0 & \hat{\sigma}_\mu \\ \hat{\sigma}_\mu^+ & 0 \end{pmatrix}, \quad (14)$$

and  $\hat{\sigma}_\mu = (1, i\sigma_k)$  with  $\sigma_k$  the Pauli  $\sigma$ -matrices, the fermionic action can be written as

$$S_F = \int d^4x \sum_{f=1}^{N_f} \begin{pmatrix} \bar{\phi}_R \\ \bar{\phi}_L \end{pmatrix} \begin{pmatrix} m_f & \hat{\sigma}_\mu(\partial_\mu + iA_\mu) \\ \hat{\sigma}_\mu^+(\partial_\mu + iA_\mu) & m_f \end{pmatrix} \begin{pmatrix} \phi_R \\ \phi_L \end{pmatrix}. \quad (15)$$

For  $N_c = 2$ , we have that  $A_\mu^T = -\tau_2 A_\mu \tau_2$  (with  $\tau_2 = \sigma_2$  in color space). Combining this with the relation  $\hat{\sigma}_\mu^* = \sigma_2 \hat{\sigma}_\mu \sigma_2$  we find

$$\bar{\phi}_L^f \hat{\sigma}_\mu^+ (\partial_\mu + iA_\mu) \phi_R^f = \phi_R^f \sigma_2 \tau_2 \hat{\sigma}_\mu (\partial_\mu + iA_\mu) \sigma_2 \tau_2 \bar{\phi}_L^f, \quad (16)$$

where we have used that  $\partial_\mu$  is anti-Hermitian and that the fermion fields are anti-commuting Grassmann variables. The fermionic action can thus be rewritten as

$$S_F(m_f = 0) = \int d^4x \sum_{f=1}^{N_f} \begin{pmatrix} \bar{\phi}_R^f \\ \sigma_2 \tau_2 \bar{\phi}_R^f \end{pmatrix} \begin{pmatrix} \hat{\sigma}_\mu(\partial_\mu + iA_\mu) & 0 \\ 0 & \hat{\sigma}_\mu(\partial_\mu + iA_\mu) \end{pmatrix} \begin{pmatrix} \phi_L^f \\ \sigma_2 \tau_2 \phi_L^f \end{pmatrix}. \quad (17)$$

Obviously the symmetry group is  $Gl(2N_f)$ . If the number of left-handed modes is not equal to the number of right-handed modes because of the anomaly, an axial  $U(1)$  is broken explicitly as for three or more colors.



The mass term is given by

$$S_m = \int d^4x \sum_{f=1}^{N_f} \left[ \begin{pmatrix} \phi_L^f \\ \sigma_2 \tau_2 \bar{\phi}_L^f \end{pmatrix} \begin{pmatrix} 0 & -m_f \sigma_2 \tau_2 \\ m_f \sigma_2 \tau_2 & 0 \end{pmatrix} \begin{pmatrix} \phi_L^f \\ \sigma_2 \tau_2 \bar{\phi}_L^f \end{pmatrix} \right. \\ \left. + \begin{pmatrix} \bar{\phi}_R^f \\ \sigma_2 \tau_2 \phi_R^f \end{pmatrix} \begin{pmatrix} 0 & m_f \sigma_2 \tau_2 \\ -m_f \sigma_2 \tau_2 & 0 \end{pmatrix} \begin{pmatrix} \bar{\phi}_R^f \\ \sigma_2 \tau_2 \phi_R^f \end{pmatrix} \right]. \quad (18)$$

Also in this case we expect maximum spontaneous chiral symmetry breaking consistent with the Vafa-Witten theorem. This means that only the subgroup of  $U(2N_f)$  that leaves both  $\bar{\phi}_R \phi_R$  and  $\bar{\phi}_L \phi_L$  invariant remains unbroken. Therefore, only the subgroup that leaves

$$\begin{pmatrix} \phi_L^f \\ \bar{\sigma}_2 \tau_2 \bar{\phi}_L^f \end{pmatrix} \begin{pmatrix} 0 & -\sigma_2 \tau_2 \\ \sigma_2 \tau_2 & 0 \end{pmatrix} \begin{pmatrix} \phi_L^f \\ \sigma_2 \tau_2 \bar{\phi}_L^f \end{pmatrix} \quad (19)$$

invariant remains unbroken ( $\bar{\phi}_R \phi_R$  is invariant under the same transformations). This is the symplectic group  $Sp(N_f)$ . The Goldstone manifold is thus given by the coset  $SU(2N_f)/Sp(N_f)$ .

For  $N_c = 2$  the Dirac-operator has the anti-unitary symmetry

$$[KC\tau_2, iD] = 0, \quad (20)$$

where  $K$  is the complex conjugation operator,  $C = \gamma_2 \gamma_4$  is the charge conjugation matrix. Because

$$(KC\tau_2)^2 = 1 \quad (21)$$

we can always find a basis such that the Dirac matrix is real for any  $D$ . The proof is along the same lines as the proof that time reversal symmetry results in real matrix elements for the Hamiltonian in quantum mechanics.

The anti-unitary symmetry would be violated in the presence of gauge fields  $B_\mu$  coupling to the axial current (which are not present in QCD). In that case the Dirac operator is given by

$$\gamma_\mu \partial_\mu + i\gamma_\mu A_\mu + \gamma_\mu \gamma_5 B_\mu, \quad (22)$$

which, because of the absence of the factor  $i$  in the  $B_\mu$ -term does not satisfy the commutation relation (20). In other words, the invariance of the Dirac operator under (20) follows from the condition  $\gamma_\mu D \gamma_\mu = 2D$  (in four dimensions). For  $N_c \geq 3$  this condition does not affect the anti-unitary symmetries, and the matrix elements of the Dirac operator are arbitrary complex numbers both with and without the  $B_\nu$  term<sup>63</sup>.

### 2.3 Dirac Operator in a Chiral Basis

It is instructive to write the Dirac operator in a chiral basis with  $n$  right-handed modes  $\phi_k^R$  and  $n+\nu$  left-handed modes  $\phi_k^L$ . Using the anti-commutation relation (7) one can easily derive that

$$\langle \phi_k^R | D | \phi_l^R \rangle = \langle \phi_k^R | \gamma_5 D \gamma_5 | \phi_l^R \rangle = -\langle \phi_k^R | D | \phi_l^R \rangle \quad (23)$$

from which it follows that  $\langle \phi_k^R | D | \phi_l^R \rangle = 0$ . Similarly,  $\langle \phi_k^L | D | \phi_l^L \rangle = 0$ , resulting in a Dirac Matrix with the structure

$$D = \begin{pmatrix} 0 & T \\ -T^\dagger & 0 \end{pmatrix}, \quad (24)$$

where  $T$  is an  $n \times (n+\nu)$  matrix. From the inspection of the secular equation one concludes that such matrix has always exactly  $\nu$  zero eigenvalues. For example, the eigenvalues of the matrix

$$D = \begin{pmatrix} 0 & a & b \\ -a^* & 0 & 0 \\ -b^* & 0 & 0 \end{pmatrix}, \quad (25)$$

are equal to 0 and  $\pm i\sqrt{a^*a + b^*b}$ . The matrix structure (24) is at the basis of the Random Matrix Theory to be discussed in section 4. A particular realization of a chiral basis is a basis of instanton zero modes which has been used extensively in the instanton liquid model of the QCD vacuum<sup>64,29</sup>

### 2.4 Lattice QCD

In lattice QCD, the gauge fields represented by unitary matrices on the links of the lattice, i.e.

$$U_{x,x+\mu} = e^{i\frac{T_a}{2}A_\mu^a(x)}, \quad (26)$$

where  $\mu$  denotes a unit vector in the direction of  $x_\mu$ . The gluonic lattice action of QCD is the plaquette action given by

$$S = \frac{1}{2} \sum_P (S_P + S_P^\dagger). \quad (27)$$

For example, the action of an elementary plaquette 1234 is given by

$$S_P = \text{Tr} U_{12} U_{23} U_{43}^{-1} U_{14}^{-1}. \quad (28)$$

This action is invariant under the local gauge transformations

$$U_{kl} \rightarrow V_k^{-1} U_{kl} V_l. \quad (29)$$

The fermion fields are represented by Grassmann valued fields on the sites. Under gauge transformations they transform according to

$$\psi_k \rightarrow U_{kl} \psi_l. \quad (30)$$

However, a lattice discretization of the Dirac action is more problematic. In a naive lattice discretization we are faced with the fermion doubling problem. This is highlighted by the Nielsen-Ninomiya theorem<sup>65</sup>, which states that a lattice discretization of chiral fermions with local interactions is not possible.

There are two widely used discretizations of the fermionic action which deal with the doubling problem at the expense of some of the symmetries of the continuum QCD action: the Kogut-Susskind or staggered action and the Wilson action. The Kogut-Susskind action is defined by

$$\begin{aligned} S^{KS} &= \frac{1}{2} \sum_{n, \mu} \eta_\mu(n) \bar{\chi}_n (U_{n, n+\mu} \chi_{n+\mu} - U_{n-\mu, n}^\dagger \chi_{n-\mu}) + m \sum_n \bar{\chi}_n \chi_n \\ &= \bar{\chi}_m D_{mn}^{KS} \chi_n, \end{aligned} \quad (31)$$

where  $\eta_\mu(n)$  is a phase factor resulting from the diagonalization of the  $\gamma$ -matrices. For  $m = 0$  and  $n_1 + n_2 + n_3 + n_4$  even, this action is invariant under the transformations

$$\bar{\chi}_n \rightarrow e^{i\theta} \bar{\chi}_n, \quad \chi_{n+\mu} \rightarrow e^{-i\theta} \chi_{n+\mu}. \quad (32)$$

For all  $n_i$  we have the invariance

$$\bar{\chi}_n \rightarrow e^{i\alpha} \bar{\chi}_n, \quad \chi_n \rightarrow e^{-i\alpha} \chi_n. \quad (33)$$

For  $m \neq 0$  this  $U(1) \times U(1)$  symmetry is broken to the second  $U(1)$  symmetry only. If we organize the Kogut-Susskind Dirac matrix according to blocks with even and odd  $n_1 + n_2 + n_3 + n_4$ , one obtains the same block structure as in the chiral representation of the continuum Dirac operator (24). This shows that that the eigenvalues of  $D^{KS}$  occur in pairs  $\pm\lambda$ .

The staggered Dirac operator is anti-Hermitian with eigenvalues  $i\lambda_k$  on the imaginary axis. The Dirac operator satisfies the sum-rule

$$\text{Tr} D^{KS} D^{KS} = \text{Tr} D^{KS} D^{KS} \big|_{U=1}. \quad (34)$$

This follows from the observation that  $U$  only occurs in the combination  $UU^{-1}$  in the left hand side of this equation. An important application of this sum rule is as a test of the accuracy of numerically calculated eigenvalues of the Dirac operator.

The Wilson Dirac action is defined by

$$\begin{aligned} S^W &= -\frac{1}{2} \sum_{n,\mu} \bar{\psi}_n^f ((r - \gamma_\mu) U_{n,n+\mu} \psi_{n+\mu} + (r + \gamma_\mu) U_{n-\mu,n}^\dagger) \psi_{n-\mu}^f + \sum_n \bar{\psi}_n^f (m + 4r) \psi_n^f \\ &= \bar{\psi}_n^f D_{nm}^W \psi_m^f. \end{aligned} \quad (35)$$

The term proportional to  $r$  was introduced by Wilson to remove the fermion doublers. However, it also destroys the  $U_A(1)$  symmetry of  $D^W$ , and the eigenvalues do not occur in pairs  $\pm\lambda$ . On the other hand, this action is invariant under the flavor group  $SU_V(N_f)$ . The Wilson Dirac operator satisfies the Hermiticity relation

$$D^{W\dagger} = \gamma_5 D^W \gamma_5 \quad (36)$$

from which it follows that  $\gamma_5 D^W$  is Hermitean. In the literature Dirac spectra of both  $D^W$  with eigenvalues scattered in the complex plane<sup>66,67,68</sup> and  $\gamma_5 D^W$  with eigenvalues on the real axis<sup>69,70</sup> have been studied (several reviews appeared recently<sup>71,72</sup>). Below we will restrict ourselves to the Hermitean Wilson Dirac operator. The Wilson Dirac operator satisfies the sum rule

$$\text{Tr} D^{W\dagger} D^W = \text{Tr} D^{W\dagger} D^W|_{U=1}. \quad (37)$$

Again this can be seen from the observation that  $U$  only occurs in the combination  $UU^{-1}$  in the l.h.s. of this equation.

The anti-unitary symmetries of the Wilson Dirac operator are the same as of the continuum Dirac operator. For  $N_c = 2$  we thus have

$$[CK\tau_2, iD^W] = 0. \quad (38)$$

For staggered fermions only the eigenvalues of the  $\gamma$  matrices appear in the Dirac operator. Since they are real they do not affect the anti-unitary symmetry. For  $N_c = 2$  we thus have

$$[K\tau_2, D^{KS}] = 0. \quad (39)$$

However,  $(K\tau_2)^2 = -1$ , and it can be shown that it is always possible to find a basis such that the matrix elements of  $D^{KS}$  can be organized into real

quaternions for any gauge field configuration. The eigenvalues of such matrix are scalar quaternions and are thus doubly degenerate. This can also easily be shown from (39). Because of this relation, if  $\phi$  is an eigenfunction with eigenvalue  $\lambda$  then  $K\tau_2\phi$  is also an eigenfunction with eigenvalue  $\lambda$ . But

$$(\phi, K\tau_2\phi) = (K\tau_2\phi, \phi)^* = ((K\tau_2)^2\phi, K\tau_2\phi) = -(\phi, K\tau_2\phi), \quad (40)$$

from which it follows that  $\phi$  and  $K\tau_2\phi$  are linearly independent. For a more detailed discussion of the symmetries of the staggered Dirac operator we refer to <sup>10,73,74</sup>.

### 2.5 The Chiral Phase Transition in QCD

It is expected that chiral symmetry will be restored above some critical temperature. This is supported both by naive arguments based on counting the total number of degrees of freedom and by lattice QCD simulations<sup>1</sup>. In the chiral limit, the order parameter for the chiral phase transition is the chiral condensate,  $\langle\bar{\psi}\psi\rangle$ . For QCD with three color and two massless quarks, it vanishes above a critical temperature of about 140 MeV. The nature of the phase transition is still under dispute. It is not yet clear whether the transition is a second order or a weak first order one<sup>1</sup>. The role of instanton field configurations has to be clarified as well<sup>75,71</sup>. However, with current progress in computational resources, these questions should be answered in the near future. The only remaining fundamental problem is the study of QCD at finite baryon density. Because of the phase of the fermion determinant, this problem cannot be resolved by means of Monte-Carlo simulations. Progress in this area requires new paradigms which make it a particularly challenging area of active research.

### 2.6 The Banks-Casher Relation and Microscopic Spectral Density

The order parameter of the chiral phase transition,  $\langle\bar{\psi}\psi\rangle$ , is nonzero only below the critical temperature or a critical chemical potential. As was shown by Banks and Casher<sup>5</sup>,  $\langle\bar{\psi}\psi\rangle$  is directly related to the eigenvalue density of the QCD Dirac operator per unit four-volume

$$\Sigma \equiv |\langle\bar{\psi}\psi\rangle| = \lim \frac{\pi\langle\rho(0)\rangle}{V}, \quad (41)$$

where the spectral density of the Dirac operator with eigenvalues  $\{\lambda_k\}$  is defined by

$$\rho(\lambda) = \langle \sum_k \delta(\lambda - \lambda_k) \rangle. \quad (42)$$

It is elementary to derive this relation. The chiral condensate is defined as the logarithmic derivative of the the partition function (8). For equal quark masses we obtain,

$$\langle \bar{\psi}\psi \rangle = -\lim \frac{1}{VN_f} \partial_m \log Z^{QCD}(m) = -\lim \frac{1}{V} \langle \sum_k \frac{2m}{\lambda_k^2 + m^2} \rangle. \quad (43)$$

If we express the sum as an integral over the average spectral density, and take the thermodynamic limit before the chiral limit, so that many eigenvalues are less than  $m$ , we recover (41). The order of the limits in (41) is important. First we take the thermodynamic limit, next the chiral limit and, finally, the field theory limit. As follows from (43), the sign of  $\langle \bar{\psi}\psi \rangle$  changes if  $m$  crosses the real axis.

An important consequence of the Bank-Casher formula (41) is that the eigenvalues near zero virtuality are spaced as

$$\Delta\lambda = 1/\rho(0) = \pi/\Sigma V. \quad (44)$$

This should be contrasted with the eigenvalue spectrum of the non-interacting Dirac operator. Then the eigenvalues are those of a free Dirac particle in a box with eigenvalue spacing equal to  $\Delta\lambda \sim 1/V^{1/4}$  for the eigenvalues near  $\lambda = 0$ . Clearly, the presence of gauge fields leads to a strong modification of the spectrum near zero virtuality. Strong interactions result in the coupling of many degrees of freedom leading to extended states and correlated eigenvalues.

Because the eigenvalues near zero are spaced as  $\sim 1/\Sigma V$  it is natural to introduce the microscopic variable

$$u = \lambda V \Sigma, \quad (45)$$

and the microscopic spectral density<sup>24</sup>

$$\rho_s(u) = \lim_{V \rightarrow \infty} \frac{1}{V\Sigma} \langle \rho(\frac{u}{V\Sigma}) \rangle. \quad (46)$$

We expect that this limit exists and converges to a universal function which is determined by the global symmetries of the QCD Dirac operator. The calculation of this universal function from QCD is the main objective of these lectures. We will calculate  $\rho_s(u)$  both from the simplest theory in this universality class which is chiral Random Matrix Theory (chRMT) and from the partial quenched chiral Lagrangian which describes the low-energy limit of the QCD partition function. We find that the two results coincide below the Thouless energy.

### 2.7 Valence Quark Mass Dependence of the Chiral Condensate

Instead of studying the Dirac spectrum it is often convenient to consider the valence quark mass dependence of the chiral condensate. In terms of the eigenvalues of the Dirac operator it is defined by<sup>76,22,23</sup>

$$\begin{aligned}\Sigma(m_v; m_1, \dots, m_{N_f}) &= \frac{1}{V} \sum_k \left\langle \frac{1}{i\lambda_k + m_v} \right\rangle \\ &= \frac{1}{V} \int d\lambda \frac{\rho(\lambda; m_1, \dots, m_{N_f})}{i\lambda + m_v}.\end{aligned}\quad (47)$$

Here,  $\langle \dots \rangle$  denotes an average with respect to the distribution of the eigenvalues.

The relation (47) can then be inverted to give  $\rho(\lambda; m_1, \dots, m_{N_f})$ . As mentioned in<sup>16</sup>, the spectral density follows from the discontinuity across the imaginary axis,

$$\text{Disc}|_{m_v=i\lambda} \Sigma(m_v) = \lim_{\epsilon \rightarrow 0} \Sigma(i\lambda + \epsilon) - \Sigma(i\lambda - \epsilon) = 2\pi \sum_k \langle \delta(\lambda + \lambda_k) \rangle = 2\pi \rho(\lambda), \quad (48)$$

where we have suppressed the dependence on the sea-quark masses.

## 3 Infrared Limit of the QCD Partition Function

### 3.1 The Chiral Lagrangian

For light quarks the low energy limit of QCD is well understood. It is given by the chiral Lagrangian describing the interactions of the pseudoscalar mesons. The reason is that pions are Goldstone bosons which are the only light degrees of freedom in a confining theory such as QCD. To lowest order in the quark masses and the momenta, the chiral Lagrangian is completely dictated by chiral symmetry and Lorentz invariance. In the case of  $N_f$  light quarks with chiral symmetry breaking according to  $SU_L(N_f) \times SU_R(N_f) \rightarrow SU_V(N_f)$  the so called Weinberg Lagrangian is given by<sup>81</sup>

$$\mathcal{L}_{\text{eff}}(U) = \frac{F^2}{4} \text{Tr}(\partial_\mu U \partial_\mu U^\dagger) - \frac{\Sigma}{2} \text{Tr}(\hat{\mathcal{M}}U + \hat{\mathcal{M}}U^\dagger), \quad (49)$$

where  $F$  is the pion decay constant,  $\Sigma$  is the chiral condensate and  $\mathcal{M}$  is the quark mass matrix. The fields  $U(x)$  are  $SU(N_f)$  matrices parametrized as

$$U = \exp(i\sqrt{2}\Pi_a t^a / F), \quad (50)$$

with the generators of  $SU(N_f)$  normalized according to  $\text{Tr} t^a t^b = \delta^{ab}$ . This chiral Lagrangian has been used extensively for the description of pion-pion scattering amplitudes.

To lowest order in the pion fields the chiral Lagrangian can be expanded as (for equal quark masses)

$$\mathcal{L}_{\text{eff}}(U) = \frac{1}{2} \partial_\mu \Pi^a \partial^\mu \Pi^a + \frac{\Sigma m}{F^2} \Pi^a \Pi^a. \quad (51)$$

This results in the pion propagator  $1/(p^2 + m_\pi^2)$  with pion masses given by the Gellmann-Oakes-Renner relation

$$m_\pi^2 = \frac{2m\Sigma}{F^2}. \quad (52)$$

In the long-wavelength limit the order of magnitude of the different terms contributing to the action of the chiral Lagrangian is given by<sup>21</sup>

$$S = \int d^4x \mathcal{L}(U) \sim L^{d-2} \Pi_{NZM}^a{}^2 + L^d \frac{\Sigma m}{F^2} (\Pi_{ZM}^a{}^2 + \Pi_{NZM}^a{}^2). \quad (53)$$

Here, the  $\Pi_{ZM}^a$  represent the zero momentum modes with no space time dependence, whereas the nonzero momentum modes are denoted by  $\Pi_{NZM}^a(x)$ . This decomposition has two immediate consequences. First, for  $\frac{\Sigma m}{F^2} \gg \frac{1}{V}$  the fluctuations of the pion fields are small and it is justified to expand  $U$  in powers of  $\Pi^a$ . Second, for

$$\frac{\Sigma m}{F^2} \ll \frac{1}{\sqrt{V}} \quad (54)$$

the fluctuations of the zero modes dominate the fluctuations of the nonzero modes, and only the contribution from the zero modes has to be taken into account for the calculation of an observable. In this limit the so called finite volume partition function is given by

$$Z_{N_f}^{\text{eff}}(\mathcal{M}, \theta) \sim \int_{U \in SU(N_f)} dU e^{V \Sigma \text{Re Tr } \mathcal{M} U e^{i\theta/N_f}}, \quad (55)$$

where the  $\theta$ -dependence follows from the  $\theta$ -dependence of the QCD partition function via the combination<sup>8</sup>  $m e^{i\theta/N_f}$ . We emphasize that any theory with the same pattern of chiral symmetry breaking as QCD can be reduced to the same extreme infrared limit.



### 3.2 Leutwyler-Smilga Sum Rules

The finite volume partition function in the sector of topological charge  $\nu$  follows by Fourier inversion according to (8). The partition function for  $\nu = 0$  is thus given by (55) with the integration over  $SU(N_f)$  replaced by an integral over  $U(N_f)$ .

The Leutwyler-Smilga sum-rules<sup>8</sup> are obtained by expanding the partition function in powers of  $m$  before and after averaging over the gauge field configurations and equating the coefficients. This corresponds to an expansion in powers of  $m$  of both the QCD partition function (4) and the finite volume partition function (55) in the sector of topological charge  $\nu$ . As an example, we consider the coefficients of  $m^2$  in the sector with  $\nu = 0$ . After performing the group integrals we find the sum-rule

$$\langle \sum' \frac{1}{\lambda_k^2} \rangle = \frac{\Sigma^2 V^2}{4N_f}, \quad (56)$$

where the prime indicates that the sum is restricted to nonzero positive eigenvalues.

By equating higher powers of  $m^2$  one can generate an infinite family of sum-rules for the eigenvalues of the Dirac operator. However, they are not sufficient to determine the Dirac spectrum. The reason is that the mass in the propagator also occurs in the fermion-determinant of the QCD partition function. However, as will be shown in the next section, the Dirac spectrum can be obtained from a chiral Lagrangian corresponding to QCD with additional bosonic and fermionic quarks<sup>16</sup>. We conclude that chiral symmetry breaking leads to correlations of the inverse eigenvalues which are determined by the underlying global symmetries.

### 3.3 The Partially Quenched QCD Partition Function

As was mentioned in previous section, the valence quark mass dependence of the chiral condensate cannot be extracted from the QCD partition function. The solution to this problem is to simultaneously introduce yet another quark species of opposite statistics<sup>16</sup>. This corresponds to a Euclidean partition function of the form

$$Z^{\text{Pq}} = \int dA \frac{\det(D + m_{v1})}{\det(D + m_{v2})} \prod_{f=1}^{N_f} \det(D + m_f) e^{-S_{YM}}, \quad (57)$$

which we will call the partially quenched or pq-QCD partition function. When  $m_{v1} = m_{v2}$  this partition function simply coincides with the original QCD partition function. However, it is now also the generator of a mass-dependent chiral condensate (see (47)) for the additional (say, fermionic) quark species. In the sector of topological charge  $\nu$  we find

$$\Sigma(m_v; m_1, \dots, m_{N_f}) = \frac{1}{V} \left. \frac{\partial}{\partial m_{v1}} \right|_{m_{v1}=m_{v2}=m_v} \log Z_\nu^{\text{pq}}, \quad (58)$$

where  $Z_\nu^{\text{pq}}$  is the partially quenched QCD partition function in the sector of topological charge  $\nu$ .

Our aim is to find the chiral Lagrangian corresponding to (57). If we are successful, we have succeeded in deriving a partition function for the extreme infrared limit of the spectrum of the QCD Dirac operator. These questions will be addressed in the next sections.

### 3.4 The Infrared Limit of QCD

If we don't write the determinants in terms of integrals over complex conjugated variables, the global flavor symmetry of the partially quenched QCD partition function (57) is broken spontaneously according to

$$Gl_R(N_f + 1|1) \times Gl_L(N_f + 1|1) \rightarrow Gl_V(N_f + 1|1) \quad (59)$$

with an axial  $U(1)$  group broken explicitly by the anomaly. Here, the groups  $Gl_R(N_f + 1|1)$ ,  $Gl_L(N_f + 1|1)$  and  $Gl_V(N_f + 1|1)$  are super-groups of matrices acting on vectors with  $N_f + 1$  fermionic components and one bosonic component. The subscript refers to right-handed (R), left-handed (L) and vector (V), respectively. The latter transformations transform the right-handed and the left-handed fermion fields in the same way. For a confining theory such as QCD the only low-lying modes are the Goldstone modes associated with the spontaneous breaking of chiral symmetry. The quark masses play the role of symmetry breaking fields.

Although the axial supergroup  $Gl_A(N_f + 1|1)$  is a symmetry group of the pq-QCD action (57) it is not necessarily a symmetry of the QCD partition function. It may be that the symmetry transformations violate the convergence of the integrals in the partition function. There are no problems for the Grassmann variables. However, the integrations over the bosonic fields are only convergent if the fields are related by complex conjugation. For this reason a  $U_A(1)$  transformation in which the bosonic fields  $\phi_R$  and  $\phi_L$  are transformed

according to a different phase factor is not a symmetry of the partition function. What is a symmetry of the partition function is the axial transformation

$$\phi_L \rightarrow e^s \phi_L, \quad \phi_L^* \rightarrow e^s \phi_L^*, \quad (60)$$

$$\phi_R^* \rightarrow e^{-s} \phi_R^*, \quad \phi_R \rightarrow e^{-s} \phi_R. \quad (61)$$

Mathematically, this symmetry group is  $Gl(1)/U(1)$ . Had we restricted ourselves to the unitary subgroup  $U(N_f + 1|1)$  of  $Gl(N_f + 1|1)$  from the start, we would have missed this class of symmetry transformations.

Taking into account the chiral anomaly, the chiral symmetry in (57) is broken spontaneously according to (59). The symmetry of the QCD partition function is thus reduced to  $Sl_V(N_f + 1|1) \oslash Gl_V(1)$  where  $\oslash$  denotes the semi-direct product. The Goldstone manifold corresponding to the symmetry breaking pattern (59) is based on the symmetric superspace  $Sl_A(N_f + 1|1)$ . In our effective partition function the terms that break the axial symmetry will be included explicitly resulting in an integration manifold given by  $Sl_A(N_f + 1|1) \otimes Gl_A(1)$ . However, this manifold is not a super-Riemannian manifold and is not suitable as an integration domain for the low energy partition function. As an integration domain we choose the maximum Riemannian submanifold of  $Gl_A(N_f + 1|1)$ . This results in a fermion-fermion block given by the compact domain  $U_A(N_f + 1)$ , whereas the boson-boson block is restricted to the non-compact domain  $Gl(1)/U(1)$ . Because of the super-trace, this compact/non-compact structure is required for obtaining a positive definite quadratic form for the mass term and the kinetic term of our low energy effective partition function<sup>82</sup>. For a detailed mathematical discussion of this construction we refer to a paper by Zirnbauer<sup>83</sup>.

To lowest order in the momenta, the infrared limit of the QCD partition function is uniquely determined by the geometry of the Goldstone manifold and Lorentz invariance. With the singlet field  $\Phi_0 \equiv \text{Str}\Phi$  fluctuating about the vacuum angle  $\theta$  with an amplitude given by the singlet mass we thus obtain the effective partition function<sup>18,19</sup>

$$\begin{aligned} Z(\theta, \hat{\mathcal{M}}) = & \int_{U \in Gl(N_f + 1|1)} dU \exp \int d^4x \left[ \frac{F^2}{4} \text{Str}(\partial_\mu U \partial_\mu U^{-1}) \right. \\ & \left. + \frac{\Sigma}{2} \text{Str}(\hat{\mathcal{M}}U + \hat{\mathcal{M}}U^{-1}) + \frac{F^2 m_0^2}{12} \left( \frac{\sqrt{2}\Phi_0}{F} - \theta \right)^2 \right]. \end{aligned} \quad (62)$$

This partition function contains terms up to order  $p^2$ . The kinetic term of the singlet field is subleading and has not been included. The supertrace (Str) and

the superdeterminant (Sdet) of a graded matrix with bosonic blocks  $a$  and  $b$  and fermionic blocks  $\sigma$  and  $\rho$  are defined as<sup>84,85</sup>

$$\text{Str} \begin{pmatrix} a & \sigma \\ \rho & b \end{pmatrix} = \text{Tra} - \text{Tr}b, \quad (63)$$

and

$$\text{Sdet} = \frac{\det(a - \sigma b^{-1} \rho)}{\det b}. \quad (64)$$

Recently, this partition function for  $N_f = 0$  was derived from a two sublattice random flux model<sup>86</sup> using the flavor-color transformation introduced by Zirnbauer<sup>87</sup>. In our language, such model is QCD at infinite coupling with  $U(N)$  gauge fields and quenched Kogut-Susskind fermions with no phase factor from the  $\gamma$  matrices. In this case, as well as in the effective partition function for Kogut-Susskind fermion, the singlet mass term is absent. In both cases the  $U(1) \times U(1)$  symmetry is broken spontaneously to  $U(1)$  instead of broken explicitly by the anomaly. The reason is that the  $U(1)$  symmetry of Kogut-Susskind fermions is an axial isospin transformation rather than the singlet  $U_A(1)$  transformation (We thank Paul Rakow and Misha Stephanov for discussions to clarify this point.).

By a generalization of an argument due to Gasser and Leutwyler<sup>21</sup> to be discussed in the next section it can be shown that for masses in the range (1) this partition function factorizes into a product over zero momentum modes and non-zero momentum modes<sup>14,16</sup>. To leading order, the mass dependence of the of the QCD partition function is thus given by

$$Z_{\text{eff}}(\theta, \hat{\mathcal{M}}) = \int_{U \in Gl(N_f+1|1)} dU e^{V \frac{\Sigma}{2} \text{Str}(\hat{\mathcal{M}}U + \hat{\mathcal{M}}U^{-1}) - \frac{F^2 m_0^2 V}{12} (\frac{\sqrt{2}\Phi_0}{F} - \theta)^2}. \quad (65)$$

The partition function in a sector of topological charge  $\nu$  follows by Fourier inversion<sup>8</sup>

$$Z_{\text{eff}}^\nu(\hat{\mathcal{M}}) = \frac{1}{2\pi} \int_0^{2\pi} d\theta e^{-i\nu\theta} Z_{\text{eff}}(\theta, \hat{\mathcal{M}}). \quad (66)$$

We perform the integration over  $\theta$  after a Hubbard-Stratonovitch transformation which linearizes the singlet mass term. Up to a mass independent factor this results in the partition function<sup>16</sup>

$$Z_{\text{eff}}^\nu(\hat{\mathcal{M}}) = \int_{U \in Gl(N_f+1|1)} dU \text{Sdet}^\nu U e^{V \frac{\Sigma}{2} \text{Str}(\hat{\mathcal{M}}U + \hat{\mathcal{M}}U^{-1})}. \quad (67)$$

### 3.5 Domains in (Partially-Quenched) Chiral Perturbation Theory

In chiral perturbation theory the different domains of validity were analyzed in detail by Gasser and Leutwyler<sup>21</sup>. A similar analysis applies to partially quenched chiral perturbation theory. The idea is as follows. The  $U$  field can be decomposed as<sup>21</sup>

$$U = U_0 e^{i\psi(x)}. \quad (68)$$

where  $U_0$  is a constant (zero-momentum) field. The kinetic term of the low-momentum components of the  $\psi$  fields can be approximated by

$$\frac{1}{2} \int d^4x \partial_\mu \psi^a \partial_\mu \psi^a \sim L^2 \psi^2. \quad (69)$$

We observe that the magnitude of the fluctuations of the  $\psi$  field are of order  $1/L$  which justifies a perturbative expansion of  $\exp(i\psi(x))$ . The fluctuations of the zero modes (i.e. constant fields), on the other hand, are only limited by the mass term

$$\frac{1}{2} V \Sigma \text{Str} \mathcal{M}(U_0 + U_0^{-1}). \quad (70)$$

For quark masses  $m \gg 1/V\Sigma$ , the field  $U_0$  fluctuates close to the identity and the  $U_0$  field can be expanded around the identity as well. This is the domain of chiral perturbation theory.

For valence quark masses in the range

$$\frac{1}{V\Sigma} \ll m_v \ll \frac{F^2}{\Sigma L^2} \quad (71)$$

the valence quark mass dependence of the chiral condensate is dominated by the zero momentum modes which can be treated perturbatively. Below we will show that in this domain chiral perturbation theory and random matrix theory coincide. In the theory of disordered mesoscopic systems it is well-known that random matrix theory is valid below an energy scale  $\sim 1/L^2$ . This will be discussed in the next section.

### 3.6 Picture from Mesoscopic Physics

In disordered mesoscopic physics it has been found that Random Matrix Theory is valid for eigenvalues separated less than the energy scale  $E_c$  (see eq. (2)). In this context  $E_c$  is defined as the inverse tunneling time of an electron

through the sample. For diffusive motion, the distance  $\Delta x$  a particle diffuses in time interval  $\Delta\tau$  is given by

$$(\Delta x)^2 = D\Delta\tau, \quad (72)$$

where  $D$  is the diffusion constant. The diffusion time through the sample is thus given by  $L^2/D$  resulting in a Thouless energy of

$$E_c = \frac{\hbar D}{L^2}. \quad (73)$$

A second energy scale that enters in mesoscopic physics is  $\hbar/\tau_e$ , where  $\tau_e$  is the elastic scattering time. Based on these two scales three different domains for the energy difference,  $\delta E$ , that enters in the two-point correlation function, can be distinguished: the ergodic domain, the diffusive domain or Altshuler-Shklovskii domain and the ballistic domain. For energy differences  $\delta E \ll E_c$  eigenvalue correlations are given by RMT. Since for time scales larger than the diffusion time, an initially localized wave packet explores the complete phase space, this regime is known as the ergodic regime. In the diffusive regime defined by  $E_c \ll \delta E \ll \hbar/\tau_e$  only part of the phase space is explored by an initially localized wave packet, resulting in the disappearance of eigenvalue correlations. In this paper we don't consider the ballistic regime with  $\delta E \gg \hbar/\tau_e$ . For an interpretation of the Thouless energy in terms of the spreading width we refer to<sup>88,89</sup>. As was shown in<sup>90,91</sup>, the spectral two-point function can be related to the semiclassical return probability which provides a simple intuitive picture of its asymptotic behavior. For other recent studies on this topic we refer to<sup>92,93,94,95,96,97,98</sup>. What has emerged from these studies is that there is a close relation between eigenvalue correlations and localization properties of the wave functions.

Based on these ideas we can interpret the Dirac spectrum as the energy levels of a system in 4 Euclidean dimensions and one artificial time dimension. The corresponding classical evolution can be easily derived from the Heisenberg equations of motion

$$\frac{dx}{d\tau} = i[x, D]. \quad (74)$$

According to the Bohigas conjecture the eigenvalue correlations are given by RMT if and only if the corresponding classical motion is chaotic. We thus conclude that the classical time evolution of quarks in the Yang-Mills gauge fields is chaotic.

These ideas can be tested by means of lattice QCD<sup>34,35</sup> and instanton liquid<sup>14</sup> simulations. In Fig. 1, we show<sup>14</sup> the number variance  $\Sigma_2(n)$ , defined as the variance of the number of levels in an interval containing  $n$  level

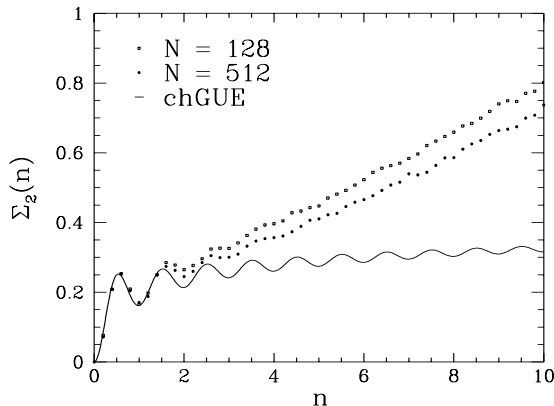


Figure 1: The number variance  $\Sigma_2(n)$  versus  $n$  approximation for an interval starting at  $\lambda = 0$ . The total number of instantons is denoted by  $N$ .

on average, versus  $n$  for eigenvalues obtained from the Dirac operator in the background of instanton liquid gauge field configurations. The chRMT result, given by the solid curve, is reproduced up to about two level spacings. In units of the average level spacing,  $\Delta = 1/\rho(0) = \pi/\Sigma V$ , the energy  $E_c$  is given by  $n_c \equiv E_c/\Delta = F^2 L^2/\pi$ . For an instanton liquid with instanton density  $N/V = 1$  we find that  $n_c \approx 0.07\sqrt{N}$ . We conclude that chRMT appears to describe the eigenvalue correlations up to the predicted scale.

In mesoscopic physics the Goldstone modes that enter in the theory of impurity scattering are known as the diffusons. The reason is that the Goldstone propagator satisfies a diffusion equation (see for example the book by Efetov<sup>85</sup>). It describes the diffusion of electrons by impurity scattering<sup>10</sup>. Similarly, the pion propagator also satisfies a diffusion equation. This can be seen by Fourier transforming the propagator with regards to the imaginary valence masses  $m_v = i\lambda$  and  $m_{v'} = i\lambda'$ ,

$$\Pi(x, \tau) = \int \frac{d^4 p}{(2\pi)^4} \int d\lambda d\lambda' \frac{e^{ipx + i\tau(\lambda + \lambda')}}{p^2 + (i\lambda + i\lambda')\Sigma/F^2}. \quad (75)$$

For  $(x, \tau) \neq 0$  this propagator satisfies the diffusion equation

$$(D\partial_x^2 - \partial_\tau)\Pi(x, \tau) = 0 \quad (76)$$

with a diffusion constant given by<sup>14,99</sup>  $D = F^2/\Sigma$ .

## 4 Calculation of Valence Quark Mass Dependence of the Chiral Condensate from QCD

### 4.1 Nonperturbative Evaluation of $\Sigma(m_v)$

In this section we calculate the valence quark mass dependence of the chiral condensate for the simplest case of  $N_f = 0$  and  $\nu = 0$  in the domain  $m_v \ll F^2/\Sigma L^2$ . In this domain the partition function is given by

$$Z(J) = \int_{U \in Gl(1|1)} dU \exp \left[ \frac{\Sigma V}{2} \text{Str} \begin{pmatrix} m_v + J & 0 \\ 0 & m_v \end{pmatrix} (U + U^{-1}) \right], \quad (77)$$

where the integration is over the maximum super-Riemannian sub-manifold of  $Gl(1|1)$ . This manifold is parametrized by

$$U = \exp \begin{pmatrix} 0 & \alpha \\ \beta & 0 \end{pmatrix} \begin{pmatrix} e^{i\phi} & 0 \\ 0 & e^s \end{pmatrix}. \quad (78)$$

The integration measure is the Haar measure which in terms of this parametrization it is given by

$$\text{Sdet} \frac{\delta U_{kl}}{\delta \phi \delta s \delta \alpha \delta \beta} d\alpha d\beta d\phi ds, \quad (79)$$

where  $\delta U \equiv U^{-1} dU$ .

It is straightforward to calculate the Berezinian going from the variables  $\delta U_{11} \delta U_{22} \delta U_{12} \delta U_{21}$  to the variables  $\delta \phi \delta s \delta \alpha \delta \beta$ . The derivative matrix is given by

$$B = \frac{\delta U_{kl}}{\delta \phi \delta s \delta \alpha \delta \beta} = \begin{pmatrix} i & 0 & \beta/2 & \alpha/2 \\ 0 & 1 & \beta/2 & \alpha/2 \\ 0 & 0 & e^{s-i\phi} & 0 \\ 0 & 0 & 0 & e^{-s+i\phi} \end{pmatrix}. \quad (80)$$

Using the definition of the graded determinant one simply finds that  $\text{Sdet} B = i$ . Up to a constant, the integration measure is thus given by  $d\phi ds d\alpha d\beta$ . In general, for  $N_f \neq 0$ , the Berezinian is more complicated<sup>84,17</sup>.

We also need

$$\frac{1}{2}(U + U^{-1}) = \begin{pmatrix} (1 + \frac{\alpha\beta}{2}) \cos \phi & \alpha(e^s - e^{-i\phi}) \\ \beta(e^{i\phi} - e^{-s}) & \cosh s(1 - \frac{\alpha\beta}{2}) \end{pmatrix}. \quad (81)$$

After differentiating with respect to the source term ( $\Sigma(m_v) = \partial_J \log Z(J)|_{J=0/V}$ ) this results in

$$\frac{\Sigma(m_v)}{\Sigma} = \int \frac{d\phi ds d\alpha d\beta}{2\pi} \cos \phi \left(1 + \frac{\alpha\beta}{2}\right) e^{x \cos \phi (1 + \frac{\alpha\beta}{2}) - x \cosh s (1 - \frac{\alpha\beta}{2})}. \quad (82)$$



With the Grassmann integral given by the coefficient of  $\alpha\beta$  we obtain

$$\frac{\Sigma(m_v)}{\Sigma} = \int \frac{ds d\phi}{4\pi} [\cos \phi + x(\cos \phi + \cosh s) \cos \phi] e^{x(\cos \phi - \cosh s)}. \quad (83)$$

Now all integrals can be expressed in terms of modified Bessel functions. We find

$$\frac{\Sigma(m_v)}{\Sigma} = I_1(x)K_0(x) + \frac{x}{2}(I_2(x)K_0(x) + I_0(x)K_0(x) + 2I_1(x)K_1(x)). \quad (84)$$

After using the recursion relation for modified Bessel functions,

$$I_2(x) = I_0(x) - \frac{2}{x}I_1(x), \quad (85)$$

we arrive at the final result<sup>22,16,17</sup>

$$\frac{\Sigma(m_v)}{\Sigma} = x(I_0(x)K_0(x) + I_1(x)K_1(x)), \quad (86)$$

where  $x = mV\Sigma$ .

This calculation can be generalized to arbitrary  $N_f$  and arbitrary  $\nu$ . The calculation for arbitrary  $N_f$  is much more complicated, but with a natural generalization of the factorized parametrization, and using some known integrals over the unitary group<sup>100</sup>, one arrives at an expression in terms of modified Bessel functions

$$\frac{\Sigma(x)}{\Sigma} = x(I_a(x)K_a(x) + I_{a+1}(x)K_{a-1}(x)), \quad (87)$$

where  $a = N_f + |\nu|$ . This result is in complete agreement<sup>17</sup> with chRMT to be discussed below.

#### 4.2 Perturbative Calculation

The valence quark mass dependence of the chiral condensate follows from (see eq. (58))

$$\Sigma(m_v) = \frac{1}{V} \partial_J \log Z_{\text{eff}}^\nu(\hat{\mathcal{M}}) \Big|_{J=0}. \quad (88)$$

In the quenched limit this results in (see eq. (62) for the definition  $S(U(x))$ )

$$\Sigma(m_v) = \int_{U(x) \in Gl(1|1)} dU(x) \frac{\Sigma V}{2} \partial_J \text{Str} \mathcal{M}(U(x) + U^{-1}(x)) e^{S(U(x))}, \quad (89)$$

Perturbatively to one loop order we can expand  $U$  around the identity, and do the usual Gaussian integrations for a flat measure. The trace of the propagator of the Goldstone bosons containing valence quarks is given by

$$\langle \pi_k^2 \rangle = \frac{1}{V} \sum_p \frac{(-1)^L}{p^2 + M_\pi^2}, \quad (90)$$

where  $L$  is 1 for a bosonic pion and 1 for a fermionic pion. The valence pion mass,  $M_\pi$ , is given by the Gell-Mann-Oakes-Renner relation

$$M_{vv} = \frac{2m_v \Sigma}{F^2}, \quad \text{or} \quad M_{vs} = \frac{(m_v + m_s) \Sigma}{F^2}, \quad \text{or} \quad M_{ss} = \frac{2m_s \Sigma}{F^2}. \quad (91)$$

The calculation of the valence quark-mass dependence of the chiral condensate using the partially quenched chiral Lagrangian is basically straightforward. The only complication is the " $\eta'$ "-mass term (the terms proportional to  $m_0^2$  in the Lagrangian). However, the quadratic form in the pion fields can be diagonalized<sup>19</sup> resulting in an analytical expression for the propagator. In the limit that the  $\eta'$  mass is much larger than the mass of the Goldstone bosons, we find<sup>50,16</sup>

$$\frac{\Sigma_v(m_v)}{\Sigma} = 1 - \frac{1}{N_f F^2} \left\{ N_f^2 \Delta(M_{sv}^2) - \Delta(M_{vv}^2) + (M_{ss}^2 - M_{vv}^2) \partial_{M_{vv}^2} \Delta(M_{vv}^2) \right\}. \quad (92)$$

where the trace of the finite volume pion propagator is given by

$$\Delta(M^2) = \frac{1}{V} \sum_p \frac{1}{p^2 + M^2}. \quad (93)$$

Here, the sum is over momenta in a box of volume  $L^4$ . From a careful analysis of the diverging momentum summations it follows that this propagator can be expanded in powers of  $M^2$

$$\Delta(M^2) = \frac{1}{M^2 L^4} - \frac{\beta_1}{L^2} + O\left(\frac{M^2}{\Lambda^2}\right), \quad (94)$$

where  $\beta_1 = 0.140461$  for a 4-dimensional hyper-cubic box, and  $\Lambda$  is the momentum cutoff<sup>101</sup>. In agreement with a naive inspection of the momentum sum, the propagator is dominated by the zero momentum term if

$$M \ll \frac{1}{L}, \quad (95)$$

or the Compton wavelength of the valence pion is much larger than the size of the box. As discussed in section (3.1) we thus find that for

$$m_v \ll \frac{F^2}{\Sigma L^2} \quad (96)$$

the valence quark mass dependence of the chiral condensate is described by the zero momentum contribution to the trace of the propagator. Let us investigate the zero momentum limit of (92) given by replacing the propagator by the first term in (94). In the chiral limit with  $m_s \rightarrow 0$  we then find

$$\begin{aligned} \Sigma_v &\sim \Sigma \left(1 - \frac{N_f}{VM_{sv}^2 F^2}\right) \\ &\sim \Sigma \left(1 - \frac{N_f}{m_v V \Sigma}\right). \end{aligned} \quad (97)$$

The nonperturbative result for  $\Sigma(m_v)$  obtained for a fixed value of the topological charge (87)  $\nu$  instead of at  $\theta = 0$  can also be expanded in powers of  $1/x \equiv 1/m_v V \Sigma$

$$\frac{\Sigma(x)}{\Sigma} \sim 1 - \frac{N_f + |\nu|}{x} + \frac{|\nu|}{x} + O\left(\frac{1}{x^3}\right), \quad (98)$$

where the term  $|\nu|/x$  results from the factor  $m^{|\nu|}$  in the partition function<sup>102</sup>. We find that to leading order in  $1/x$  the valence quark mass dependence of the chiral condensate does not depend on the topological charge and agrees with chiral perturbation theory.

The result for the valence quark mass dependence of the chiral condensate (92) is valid in the diffusive domain as well. In that case it is possible to rederive and to extend results by Smilga and Stern<sup>103</sup> for the slope of the Dirac spectrum.

### 4.3 Two-Point Correlation Function

Let us do a perturbative calculation of the two-point function in the domain that is dominated by the zero-momentum modes, i.e. for valence quark masses well below  $F^2/\Sigma L^2$ . The generating function is defined by

$$Z(J, J') = \int_{U \in Gl(2|2)} dU e^{S(U)}, \quad (99)$$

where the action is given by

$$S(U) = \frac{\Sigma V}{2} \text{Str} \begin{pmatrix} m+J & 0 & 0 & 0 \\ 0 & m'+J' & 0 & 0 \\ 0 & 0 & m & 0 \\ 0 & 0 & 0 & m' \end{pmatrix} (U + U^{-1}). \quad (100)$$

The spectral two-point correlation function follows from the partition function by<sup>16</sup>

$$\langle \rho(\lambda) \rho(\lambda') \rangle = \frac{1}{4\pi^2} \text{Disc} \partial_J \partial_{J'} Z(J, J')|_{J=0, J'=0, m=i\lambda, m'=i\lambda'}. \quad (101)$$

We are interested in the discontinuity of the connected part of the correlation function. The only contribution is from mesons containing a valence quark with mass  $m$  and a valence quark with mass  $m'$ . If we expand  $U \equiv \exp i\sqrt{2}\Pi_a T^a / F$  in powers of  $\Pi_a T^a / F$  we find that the connected spectral two-point function

$$\langle \rho(\lambda) \rho(\lambda') \rangle_c = \frac{\Sigma^2}{F^4 4\pi^2} \text{Disc}|_{m=i\lambda, m'=i\lambda'} \frac{1}{M_{vv'}^2}, \quad (102)$$

has been expressed in terms of the discontinuity of the valence pion susceptibility. To obtain this result we have used among others that

$$\text{Str} \begin{pmatrix} 1 & 0 & 0 & 0 \\ 0 & 0 & 0 & 0 \\ 0 & 0 & 0 & 0 \\ 0 & 0 & 0 & 0 \end{pmatrix} T_a T^a = \frac{1}{2}, \quad (103)$$

and the super-symmetry of the partition function. To calculate the discontinuity we wish to remind the reader that

$$M_{vv'} = \frac{(|m| + |m'|)\Sigma}{F^2}, \quad (104)$$

where  $|m| = \sqrt{\overline{m^2}}$ . We finally find

$$\langle \rho(\lambda) \rho(\lambda') \rangle_c = \frac{1}{2\pi^2} \left( \frac{1}{(\lambda + \lambda')^2} + \frac{1}{(\lambda - \lambda')^2} \right), \quad (105)$$

which agrees with the asymptotic result for the spectral correlation function<sup>104</sup> for the chiral Random Matrix Theory to be discussed next.

## 5 Chiral Random Matrix Theory

### 5.1 Definition of the Model

The chiral random matrix partition function with the global symmetries of the QCD partition function as input is defined by<sup>24,25</sup>

$$Z_{\beta}^{\nu}(\mathcal{M}) = \int DW \prod_{f=1}^{N_f} \det(\mathcal{D} + m_f) e^{-\frac{N\beta}{4} \Sigma \text{Tr} W^{\dagger} W}, \quad (106)$$

where

$$\mathcal{D} = \begin{pmatrix} 0 & iW \\ iW^{\dagger} & 0 \end{pmatrix}, \quad (107)$$

and  $W$  is a  $n \times m$  matrix with  $\nu = |n - m|$  and  $N = n + m$ . As is the case in QCD, we assume that the equivalent of the topological charge  $\nu$  does not exceed  $\sqrt{N}$ , so that, to a good approximation,  $n = N/2$ . Then the parameter  $\Sigma$  can be identified as the chiral condensate and  $N$  as the dimensionless volume of space time (Our units are defined such that the density of the modes  $N/V = 1$ ). The matrix elements of  $W$  are either real ( $\beta = 1$ , chiral Gaussian Orthogonal Ensemble (chGOE)), complex ( $\beta = 2$ , chiral Gaussian Unitary Ensemble (chGUE)), or quaternion real ( $\beta = 4$ , chiral Gaussian Symplectic Ensemble (chGSE)). For QCD with three or more colors and quarks in the fundamental representation the matrix elements of the Dirac operator are complex and we have  $\beta = 2$ . For  $N_c = 2$  and quarks in the fundamental representation the situation is more interesting. As discussed in section (2.4) it is always possible to find a basis for which the matrix elements of the continuum Dirac operator are real for all gauge fields. Then the Dyson index of the corresponding chRMT is  $\beta = 1$ . For Kogut-Susskind fermions in this case the anti-unitary symmetry is different (see section (2.4)) and the matrix elements of the Dirac operator can be organized into real quaternions corresponding to a chRMT with  $\beta = 4$ . For gauge fields in the adjoint representation the gauge fields are real resulting in an anti-unitary symmetry also corresponding to the class  $\beta = 4$  for any value of  $N_c$ .

The reason for choosing a Gaussian distribution of the matrix elements is its mathematical simplicity. This model can be generalized to arbitrary potential

$$\text{Tr} W^{\dagger} W \rightarrow \text{Tr} V(W^{\dagger} W) \quad (108)$$

where  $V(x)$  is such that the resulting probability distribution is well defined. In section (5.4) we will argue that the interesting properties of chRMT do not depend on the choice of  $V(x)$ .

Below we will also discuss the invariant or Dyson-Wigner Random Matrix Ensembles. They are defined as ensembles of Hermitean matrices  $\{H\}$  with independently Gaussian distributed matrix elements, i.e. with probability distribution given by

$$P(H) \sim e^{-\frac{N\beta}{2}\text{Tr}H^\dagger H}. \quad (109)$$

Depending on the anti-unitary symmetry, the matrix elements are real, complex or quaternion real. They are called the Gaussian Orthogonal Ensemble (GOE), the Gaussian Unitary Ensemble (GUE) and the Gaussian Symplectic Ensemble (GSE), respectively. Each ensemble is characterized by its Dyson index  $\beta$  which is defined as the number of independent variables per matrix element. For the GOE, GUE and the GSE we thus have  $\beta = 1, 2$  and  $4$ , respectively.

Together with the Wigner-Dyson ensembles and the superconducting random matrix ensembles<sup>105</sup> the chiral ensembles can be classified according to the Cartan classification of large symmetric spaces<sup>83</sup>.

## 5.2 Symmetries

From the structure of the determinant, it follows immediately that the chiral random matrix partition function has the same global flavor and  $U_A(1)$  symmetries as the QCD partition function.

It can be shown that in the domain (1) the random matrix partition function can be mapped onto the effective finite volume partition function<sup>24</sup>. We will discuss such derivation in section (7.3) where we extend this model to finite temperature. The most detailed studies to this model were performed in the quenched limit by means of the supersymmetric method<sup>77,78,79,80</sup>. In that case the chRMT partition function can be mapped onto a super-symmetric nonlinear  $\sigma$ -model.

In this model chiral symmetry is broken spontaneously with chiral condensate given by  $\Sigma = \lim_{N \rightarrow \infty} \pi \rho(\lambda \rightarrow 0)/N$ , where  $N$  is interpreted as the (dimensionless) volume of space time. For complex matrix elements ( $\beta = 2$ ), which is appropriate for QCD with three or more colors and fundamental fermions, the symmetry breaking pattern is<sup>106</sup>  $SU(N_f) \times SU(N_f)/SU(N_f)$ . For  $\beta = 1$  and  $4$  the symmetry breaking pattern is  $SU(2N_f)/Sp(N_f)$  and  $SU(N_f)/O(N_f)$  respectively<sup>106</sup>, the same as in QCD<sup>62</sup>.

Finally, one of the reasons for the mathematical simplicity of this model is that it has more symmetry than the QCD partition function. The chRMT partition function is invariant with respect to the unitary transformation

$$W \rightarrow UWV^{-1}. \quad (110)$$

Since an arbitrary complex matrix can be decomposed as

$$W = U\Lambda V^{-1}, \quad (111)$$

with  $\Lambda$  a diagonal matrix and  $U$  and  $V$  unitary matrices, the chRMT partition function for arbitrary potential  $V(\lambda)$  can be expressed in terms of the eigenvalues  $\lambda_k$  as

$$Z_\beta^\nu(\mathcal{M}) = \int d\lambda |\Delta(\lambda_k^2)|^\beta \prod_k \lambda_k^{\beta\nu+\beta-1} \prod_f m_f^\nu \prod_{f,k} (\lambda_k^2 + m_f^2) e^{-\frac{N\beta}{4} \sum_k V(\lambda_k^2)}, \quad (112)$$

where the Vandermonde determinant is defined by

$$\Delta(\lambda_k^2) = \prod_{k < l} (\lambda_k^2 - \lambda_l^2). \quad (113)$$

This result greatly simplifies the mathematical treatment of the chRMT partition function. For example, it allows us to use the orthogonal polynomial method. We wish to point out that for  $\beta = 2$  and  $m_f = 0$  the ratio of the partition function and  $m^{N_f|\nu|}$  depends only on  $\nu$  through the combination  $N_f + |\nu|$ . This duality between flavor and topology can be understood more directly via Itzykson-Zuber integrals<sup>107,108</sup>.

### 5.3 Properties of the Random Matrix Model

The average spectral density that can be derived from (106) has the familiar semi-circular shape. As can be easily derived by means of the orthogonal polynomial method, the microscopic spectral density for the chGUE is given by<sup>109,104,25</sup>

$$\rho_S(u) = \frac{u}{2} (J_a^2(u) - J_{a+1}(u)J_{a-1}(u)), \quad (114)$$

where  $a = N_f + |\nu|$ . The valence quark mass dependence of the chiral condensate follows from integration over the microscopic spectral density. If we use the microscopic variable  $u = \lambda V \Sigma$  as new integration variable, equation (47) can be rewritten as

$$\frac{\Sigma(m_v)}{\Sigma} = \int_0^\infty du \frac{2u du}{u^2 + (m_v V \Sigma)^2} \frac{1}{V \Sigma} \rho\left(\frac{u}{V \Sigma}\right). \quad (115)$$

In the thermodynamic limit, the spectral density can be replaced by the microscopic spectral density (114). The integrals over the Bessel functions are known

and result in the following expression for the valence quark mass dependence of the chiral condensate<sup>22</sup>

$$\frac{\Sigma(x)}{\Sigma} = x(I_a(x)K_a(x) + I_{a+1}(x)K_{a-1}(x)), \quad (116)$$

where  $a = N_f + |\nu|$ ,  $x = m_v V \Sigma$  and  $I_a$  and  $K_a$  are modified Bessel functions. This result is in perfect agreement with the result obtained from the partially quenched chiral Lagrangian given in eq. (87). The spectral correlations near  $\lambda = 0$  can also be expressed in terms of Bessel functions<sup>104</sup>, whereas in the bulk of the spectrum they are given by the invariant random matrix ensembles<sup>110,111</sup>. The microscopic spectral density and the microscopic spectral correlations can also be derived for  $\beta = 1$  and  $\beta = 4$  but these two cases are mathematically much more complicated. Many other properties of the chRMT partition function have been calculated. Among others, we mention the distribution of the smallest eigenvalue<sup>112,113</sup> and the microscopic spectral density in the presence of nonzero quark masses<sup>113,114,115,116</sup>. For more discussion of the chRMT partition function we refer to<sup>107</sup>.

#### 5.4 Universality

The aim of universality studies is to identify observables that are stable against deformations of the random matrix ensemble. Not all observables have the same degree of universality. For example, a semicircular average spectral density is found for random matrix ensembles with independently distributed matrix elements with a finite variance. However, this spectral shape does not occur in nature, and it is thus not surprising that it is only found in a rather narrow class of random matrix ensembles. What is surprising is that the *microscopic* spectral density and the *microscopic* spectral correlators are stable with respect to a much larger class of deformations<sup>117,118,119,120,121,122,123,124,125,126</sup>. Two different types of deformations have been considered, those that maintain the unitary invariance of the partition functions and those that break the unitary invariance.

In the first class, the Gaussian probability distribution is replaced by  $P(W) \sim \exp(-N \sum_{k=1}^{\infty} a_k \text{Tr}(W^\dagger W)^k)$ . For a potential with only  $a_1$  and  $a_2$  different from zero it was shown<sup>119</sup> that the microscopic spectral density is independent of  $a_2$ . A general proof valid for arbitrary potential and all correlation functions was given by Akemann et al.<sup>120</sup>. The essence of the proof is a remarkable generalization of the identity for the Laguerre polynomials,  $\lim_{n \rightarrow \infty} L_n(x/n) = J_0(2\sqrt{x})$ , to orthogonal polynomials determined by an arbitrary potential. It was proved by taking the continuum limit of the recursion relation for orthogonal polynomials.



In the second class, an arbitrary fixed matrix is added to  $W$  in the Dirac operator (107). It has been shown that the microscopic spectral density and the microscopic spectral correlations remain unaffected<sup>78,79,80</sup> for parameter values that completely modify the average spectral density.

Microscopic universality for deformations that affect the macroscopic spectral density implies the existence of a scale beyond which universality breaks down. It can be interpreted naturally in terms of the spreading width<sup>88</sup> which is the equivalent of the Thouless energy.

Based on the general form of the pqChPT partition function one could argue that universality of the microscopic correlators in chRMT is automatic. However, one really has to show the stability of the effective partition function with respect to variations of the distribution of matrix elements. For the Wigner-Dyson ensembles the stability of the saddle-point manifold was demonstrated in<sup>118</sup>.

For reasons of mathematical simplicity, most universality proofs have been performed for the  $\beta = 2$  ensembles. Recently, we have attempted to prove universality by establishing relations between the kernels for the  $\beta = 1$  and  $\beta = 4$  correlation functions and the kernel for the  $\beta = 2$  correlation functions. For the Gaussian ensembles such relations are exact identities<sup>127</sup>. However, for an arbitrary potential they are only valid asymptotically<sup>128,129</sup>.

There are many other results related to the universality of chRMT. We mention recent results in QCD in three dimensions<sup>120,130,131</sup>, results for Dirac operators satisfying the Ginsparg-Wilson relation<sup>132</sup>, relations between the microscopic spectral density and partition functions with two additional flavors<sup>133</sup>.

## 6 Chiral RMT as an Exact Theory for the Fluctuations of Dirac Eigenvalues

### 6.1 Statistical Analysis of Spectra

Spectra for a wide range of complex quantum systems have been studied both experimentally and numerically (a excellent recent review was given by Guhr, Müller-Groeling and Weidenmüller<sup>7</sup>). One basic observation is that the scale of variations of the average spectral density and the scale of the spectral fluctuations separate. This allows us to unfold the spectrum, i.e. we rescale the spectrum in units of the local average level spacing. Specifically, the unfolded spectrum is given by

$$\lambda_k^{\text{unf}} = \int_{-\infty}^{\lambda_k} \langle \rho(\lambda') \rangle d\lambda', \quad (117)$$

with unfolded spectral density

$$\rho_{\text{unf}}(\lambda) = \sum_k \delta(\lambda - \lambda_k^{\text{unf}}). \quad (118)$$

The fluctuations of the unfolded spectrum can be measured by suitable statistics. We will consider the nearest neighbor spacing distribution,  $P(S)$ , and moments of the number of levels in an interval containing  $n$  levels on average. In particular, we will consider the number variance,  $\Sigma_2(n)$ , and the first two cumulants,  $\gamma_1(n)$  and  $\gamma_2(n)$ . Another useful statistic is the  $\Delta_3(n)$ -statistic introduced by Dyson and Mehta<sup>134</sup>. It is related to  $\Sigma_2(n)$  via a smoothening kernel. The advantage of this statistic is that its fluctuations as a function of  $n$  are greatly reduced. Both  $\Sigma_2(n)$  and  $\Delta_3(n)$  can be obtained from the pair correlation function.

Analytical results for all spectral correlation functions have been derived for each of the three ensembles<sup>135</sup> via the orthogonal polynomial method. We only quote the most important results. The nearest neighbor spacing distribution, which is known exactly in terms of a power series, is well approximated by

$$P(S) \sim S^\beta \exp(-a_\beta S^2), \quad (119)$$

where  $a_\beta$  is a constant of order one. The asymptotic behavior of  $\Sigma_2(n)$  and  $\Delta_3(n)$  is given by

$$\Sigma_2(n) \sim (2/\pi^2 \beta) \log n \quad \text{and} \quad \Delta_3(n) \sim \beta \Sigma_2(n)/2. \quad (120)$$

Characteristic features of random matrix correlations are level repulsion at short distances and a strong suppression of fluctuations at large distances.

For uncorrelated eigenvalues the level repulsion is absent and one finds

$$P(S) = \exp(-S), \quad (121)$$

and

$$\Sigma_2(n) = n \quad \text{and} \quad \Delta_3(n) = n/15. \quad (122)$$

## 6.2 Results for Spectral Correlation Functions

Recently, lattice QCD Dirac spectra were calculated and analyzed by a number of different groups. It was found that spectral correlations below a given scale are given by chRMT, whereas above this scale, deviations from chRMT due

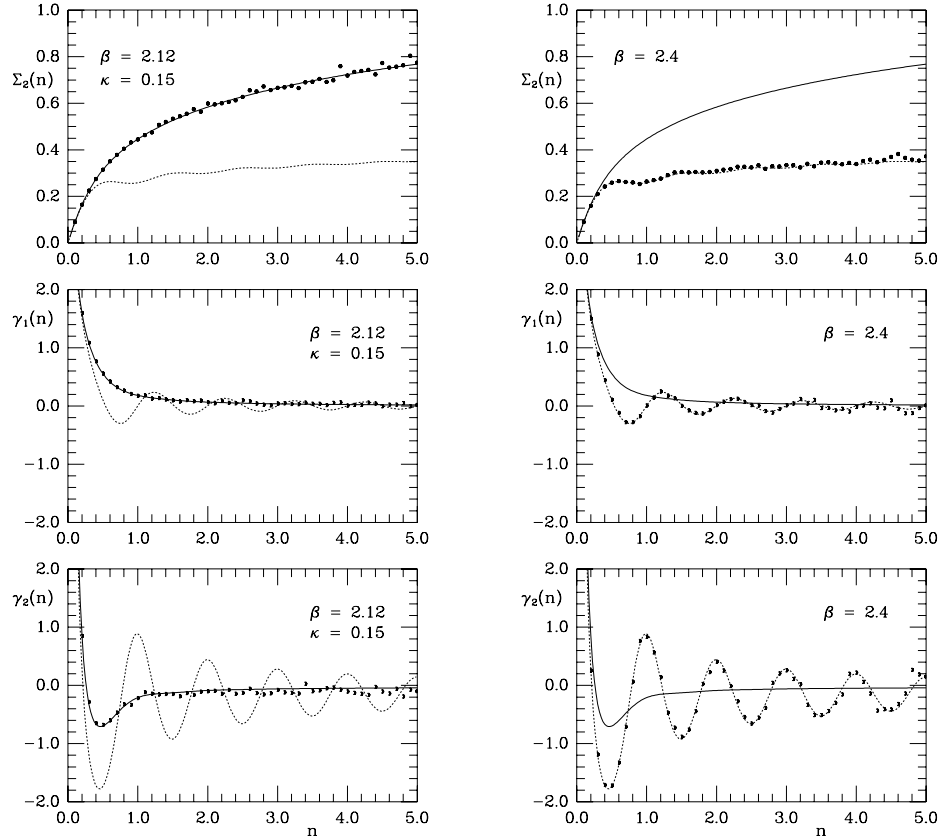


Figure 2: The number variance,  $\Sigma_2(n)$  and the first two cumulants,  $\gamma_1(n)$  and  $\gamma_2(n)$  as a function of  $n$ .

to the nonzero momentum excitations were observed. <sup>30,22,23,31,32,33,34,35,36 37,38,39,40,41,42,48,45 24,49,14,15</sup>

The first complete Dirac spectra on relatively large lattices were obtained by Kalkreuter<sup>136</sup> who calculated *all* eigenvalues of the  $N_c = 2$  Dirac operator both for Kogut-Susskind (KS) fermions and Wilson fermions for lattices as large as  $12^4$ . In both cases, the Dirac matrix was tri-diagonalized by Cullum's and Willoughby's Lanczos procedure<sup>137</sup> and diagonalized with a standard QL algorithm. This improved algorithm makes it possible to obtain *all* eigenvalues. This allows us to test the accuracy of the eigenvalues by means of sum-rules for the sum of the squares of the eigenvalues of the lattice Dirac operator (see

eqs. (34, 37)). Typically, the numerical error in the sum rule is of order  $10^{-8}$ .

Results for the spectral correlations for eigenvalues calculated by Kalkreuter<sup>136</sup> both for KS and Wilson fermions are shown in Fig. 2. The simulations for KS fermions were performed for 4 dynamical flavors with  $ma = 0.05$  on a  $12^4$  lattice (the lattice spacing is denoted by  $a$ ). The simulations for Wilson fermions were done for two dynamical flavors on an  $8^3 \times 12$  lattice.

The results for  $\Sigma_2(n)$ ,  $\gamma_1(n)$  and  $\gamma_2(n)$  obtained by spectral averaging show an impressive agreement with the RMT predictions. In the context of RMT it has been shown that spectral averages and ensemble averages coincide<sup>138</sup>. This property is known as spectral ergodicity.

Spectra for different values of  $\beta$  have been analyzed as well. It is probably no surprise that random matrix correlations are found at stronger couplings. What is surprising, however, is that even in the weak-coupling domain ( $\beta = 2.8$ ) the eigenvalue correlations are in complete agreement with Random Matrix Theory.

In the case of three or more colors with fundamental fermions, both the Wilson and Kogut-Susskind Dirac operator do not possess any anti-unitary symmetries. Therefore, our conjecture is that in this case the spectral correlations in the bulk of the spectrum of both types of fermions can be described by the GUE. This was recently confirmed for a wide range of  $\beta$ -values both below and above the deconfinement phase transition<sup>39,45</sup>.

As far as correlations in the bulk of the spectrum are concerned, in the case of two fundamental colors the continuum theory and Wilson fermions are in the same universality class. It is an interesting question of how spectral correlations of KS fermions evolve in the approach to the continuum limit. Certainly, the Kramers degeneracy of the eigenvalues remains. However, since Kogut-Susskind fermions represent 4 degenerate flavors in the continuum limit, the Dirac eigenvalues should obtain an additional two-fold degeneracy. We are looking forward to more work in this direction.

### 6.3 Correlations near Zero Virtuality

Spectral ergodicity cannot be exploited in the study of the microscopic spectral density and, in order to gather sufficient statistics, a large number of independent spectra is required. One way to proceed is to generate instanton-liquid configurations which can be obtained much more cheaply than lattice QCD configurations. Results of such analysis<sup>49</sup> show that for  $N_c = 2$  with fundamental fermions the microscopic spectral density is given by the chGOE. For  $N_c = 3$  it is given by the chGUE. One could argue that instanton-liquid configurations can be viewed as smoothened lattice QCD configurations. Roughening

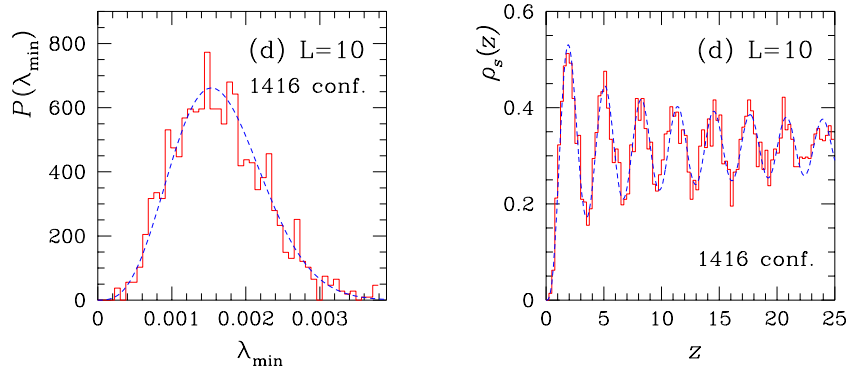


Figure 3: The distribution of the smallest eigenvalue (left) and the microscopic spectral density (right) for two colors and  $\beta = 2.0$ .

such configurations will only improve the agreement with Random Matrix Theory. Recently, these expectations were confirmed by lattice QCD simulations<sup>31</sup>. Results for 1416 quenched  $SU(2)$  Kogut-Susskind Dirac spectra on a  $10^4$  lattice are shown in Fig. 3. We show both the distribution of the smallest eigenvalue (left) and the microscopic spectral density (right). The results<sup>139</sup> for the chGSE are represented by the dashed curves.

Agreement of the microscopic spectral density with chRMT for  $N_c = 3$  was first demonstrated by means of the valence quark mass dependence of the chiral condensate<sup>22</sup>. Recently, these results were confirmed by the calculation of complete Dirac spectra<sup>41,42,48</sup>. Other recent interesting results are the calculation of the microscopic spectral density for the Dirac operator in the adjoint representation<sup>43</sup> and results for the distribution of the smallest Dirac eigenvalue at nonzero topological charge obtained by means of the overlap formalism<sup>44</sup>.

#### 6.4 The Valence Quark Mass Dependence of the Chiral Condensate

The microscopic spectral density near zero virtuality was first studied in terms of the valence quark mass dependence of the chiral condensate. The lattice data for  $\Sigma(m_v)$  were obtained by the Columbia group<sup>76</sup> for two dynamical flavors with sea-quark mass  $ma = 0.01$  and  $N_c = 3$  on a  $16^3 \times 4$  lattice. In Fig. 4 we plot the ratio  $\Sigma(m_v)/\Sigma$  as a function of  $x = m_v V \Sigma$  (the 'volume'  $V$  is equal to the total number of Dirac eigenvalues), and compare the results with the universal curves obtained from pq-QCD and chRMT (see eq. (87)).

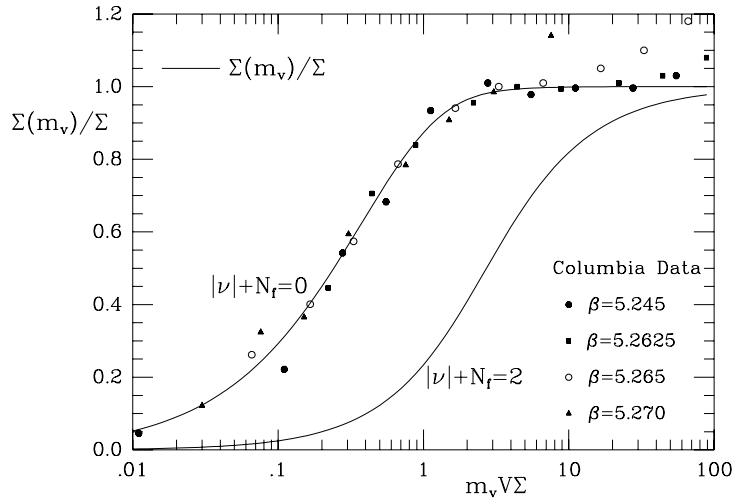


Figure 4: The valence quark mass dependence of the chiral condensate  $\Sigma(m)$  plotted as  $\Sigma(m_v)/\Sigma$  versus  $m_v V \Sigma$ . The dots and squares represent lattice results by the Columbia group<sup>76</sup> for values of  $\beta$  as indicated in the label of the figure.

We observe that the lattice data for different values of  $\beta$  fall on a single curve. Moreover, in the mesoscopic range this curve coincides with the random matrix prediction for  $N_f = \nu = 0$ . Of course this is no surprise. In the region where valence quark mass is much less than the current quark mass, the fermion determinant has no bearing on the Dirac spectrum and we have effectively  $N_f = 0$ . On a lattice the zero mode states and a much larger number of nonzero modes states are completely mixed, and therefore it is not surprising that the effective topological charge that reproduces the lattice results is equal to zero.

## 7 Chiral Random Matrix Theory as a Schematic Model for the Dirac Spectrum

### 7.1 Introduction

Up to now we have mainly focussed on chiral Random Matrix Theory as an exact theory for correlations of QCD Dirac spectra on the microscopic scale. However, in the literature one finds another important application of RMT, namely as a schematic model for a disordered system. Two well-known examples in this category are the Anderson model for localization<sup>140</sup> and RMT applied to the theory of random surfaces in connection with quantum gravity

<sup>141</sup>. In this section we will study chiral random matrix theory as a *schematic* model of the chiral phase transition at nonzero temperature and chemical potential.

## 7.2 chRMT at Nonzero Temperature

In order to obtain a chiral random matrix model for QCD at nonzero temperature we first separate the Dirac operator in two pieces

$$D = \tilde{D} + \gamma_0 \partial_0. \quad (123)$$

In a chiral basis with basis functions given by

$$\psi_{kn}(x) = \phi_k(\vec{x}) e^{-\frac{2\pi i}{\beta}(n+\frac{1}{2})x_0} \quad (124)$$

the matrix corresponding to  $\gamma_0 \partial_0$  is block diagonal with nonzero matrix elements given by the Matsubara frequencies. In our model we only keep the lowest Matsubara frequencies  $\pm\pi T$ . We expect that this is a reasonable approximation in the neighborhood of the critical temperature and beyond. The matrix corresponding to  $\tilde{D}$  is replaced by a chiral random matrix.

The chRMT Dirac operator at  $T \neq 0$  is thus given by <sup>51,52</sup>

$$D^{RMT} = \begin{pmatrix} 0 & iW \\ iW^\dagger & o \end{pmatrix} + \begin{pmatrix} 0 & i\Omega_T \\ i\Omega_T & 0 \end{pmatrix}, \quad (125)$$

where  $\Omega_T$  is given by

$$\Omega_T = \begin{pmatrix} \pi T \mathbf{1} & 0 \\ 0 & -\pi T \mathbf{1} \end{pmatrix}, \quad (126)$$

and  $\mathbf{1}$  is a unit matrix.

If we note that the probability distribution of the random matrix ensemble is invariant under  $W \rightarrow UWV^{-1}$  and use the equivalent of  $i\sigma_1\sigma_3\sigma_2 = 1$ , the random matrix Dirac operator can be simplified to

$$D(T) = \begin{pmatrix} 0 & iW + \pi iT \mathbf{1} \\ iW^\dagger + \pi iT \mathbf{1} & 0 \end{pmatrix}. \quad (127)$$

Notice that the dimension of the identity matrix in eqs. (126) and (127) differs by a factor 2.

Our finite temperature chiral random matrix model is thus given by

$$Z(\nu, N_f) = \int dW \det^{N_f}(D(T) + m) e^{-n\Sigma^2 \text{Tr} W W^\dagger}. \quad (128)$$

In the next we will perform a saddle point analysis of this model.

### 7.3 Analytical Solution

In this section we evaluate the partition function (106) using methods which are standard in the supersymmetric formulation of random matrix theory<sup>11,12</sup>. For simplicity we consider the model for  $\beta = 2$  and choose a diagonal mass matrix with equal quark masses. The first step is to perform the average over  $W$  by performing a gaussian integral. This leads to a four-fermion interaction. After averaging over the matrix elements of the Dirac operator, the partition function becomes

$$Z(\nu, N_f) = \int \mathcal{D}\psi^* \mathcal{D}\psi \exp\left[ -\frac{1}{n\Sigma^2} \psi_{Lk}^{f*} \psi_{Ri}^f \psi_{Ri}^{g*} \psi_{Lk}^g + m \psi_{Ri}^{f*} \psi_{Ri}^f + m \psi_{Lk}^{f*} \psi_{Lk}^f \right. \\ \left. - i\pi T (\psi_{Ri}^{f*} \psi_{Li}^f + \psi_{Lk}^{f*} \psi_{Rk}^f) \right]. \quad (129)$$

The four-fermion terms can be written as the difference of two squares. Each square can be linearized by

$$\exp(-AQ^2) \sim \int d\sigma \exp\left(-\frac{\sigma^2}{4A} - iQ\sigma\right). \quad (130)$$

The different  $Q$  variables, can be combined into a single complex  $N_f \times N_f$  matrix,  $A$ , resulting in

$$Z(\nu, N_f) = \int \mathcal{D}A \mathcal{D}\psi \mathcal{D}\psi^* \exp\left[-\frac{n\Sigma^2\beta}{2} \text{Tr} A A^\dagger \right. \\ \left. - i\psi_{Lk}^{f*} \psi_{Lk}^g (A + m) - i\psi_{Ri}^{f*} \psi_{Ri}^g (A^\dagger + m) - i\pi T (\psi_{Ri}^{f*} \psi_{Li}^f + \psi_{Lk}^{f*} \psi_{Rk}^f) \right]. \quad (131)$$

Note that the temperature-dependent term can be rewritten as

$$- \frac{i\pi T}{2} \begin{pmatrix} \psi_L \\ \psi_L^* \end{pmatrix} \begin{pmatrix} 0 & -\mathbf{1} \\ \mathbf{1} & 0 \end{pmatrix} \begin{pmatrix} \psi_R \\ \psi_R^* \end{pmatrix} + (L \longleftrightarrow R). \quad (132)$$

Using this, the fermionic integrals can be performed, and the partition function with  $|\nu|$  more left-handed modes than right-handed modes is given by

$$Z(\nu, N_f) = \int \mathcal{D}A \exp\left[-\frac{n\Sigma^2\beta}{2} \text{Tr} A A^\dagger\right] \det^{|\nu|}(A + m) \det^n \begin{pmatrix} A + m & -\pi iT \\ -\pi iT & A^\dagger + m \end{pmatrix}. \quad (133)$$

Here,  $A$  is an arbitrary complex matrix and  $m$  is proportional to the identity matrix.



The chiral condensate is defined by

$$\langle \bar{\psi}\psi \rangle = -\frac{1}{2nN_f} \partial_m \log Z \quad , \quad (134)$$

For  $n \rightarrow \infty$  it can be evaluated with the aid of a saddle point approximation. The saddle point equations are given by

$$-\frac{n\beta\Sigma^2}{2}A + n(A+m)((A^\dagger + m)(A+m) + \pi^2 T^2)^{-1} = 0 \quad . \quad (135)$$

An arbitrary complex matrix can be diagonalized by performing the decomposition

$$A = U\Lambda V^{-1}, \quad (136)$$

with all eigenvalues positive and  $U$  and  $V$  unitary matrices. We find that the solution of (135) yields  $U = V = 1$  with eigenvalues  $\Lambda_k$  given by the positive roots of

$$\Sigma^2 \Lambda_k ((\Lambda_k + m)^2 + \pi^2 T^2) - \Lambda_k - m = 0 \quad . \quad (137)$$

In order to calculate the condensate, we express the derivative of the partition function in (3.10) in terms of an average over  $A$ ,

$$|\langle \bar{\psi}\psi \rangle| = \frac{1}{2nN_f} \langle \text{Tr} \begin{pmatrix} A & -\pi iT \\ -\pi iT & A^\dagger \end{pmatrix}^{-1} \rangle \quad . \quad (138)$$

Below  $T_c$  and for  $m \rightarrow 0$  we find from the saddle point equation,

$$|\langle \bar{\psi}\psi \rangle| = \Sigma(1 - \pi^2 T^2 \Sigma^2)^{1/2} \quad . \quad (139)$$

In the chiral limit we thus find a critical point at

$$T_c = \frac{1}{\pi\Sigma} \quad . \quad (140)$$

Note that the dimensions are matched after including the mode density  $N/V = 1$ . Here, and elsewhere, our convention is that  $N = 2n$ . At  $T_c$  the solution of the saddle point equation develops a non-analytic dependence on  $m$  resulting in the condensate

$$|\langle \bar{\psi}\psi \rangle| = \Sigma^{\frac{4}{3}} m^{\frac{1}{3}} \quad . \quad (141)$$

Therefore, we reproduce the mean field value for the critical exponent  $\delta = 3$ .

It is also possible to obtain an analytical expression for the spectral density of this model as a function of the critical temperature. It can be obtained by solving the Schwinger-Dyson equations for the resolvent of the model<sup>51</sup> or from the observation that the solution of (135) does not depend on the number of flavors. For  $N_f \rightarrow 0$  the spectral density is then obtained from the discontinuity of the chiral condensate across the real  $m$ -axis<sup>53</sup>. The spectral density thus follows from the solution of a cubic equation. The zero temperature limit is a semicircle whereas the high temperature limit is given by two semi-circles separated by  $2\pi T$ .

#### 7.4 *chRMT at Nonzero Chemical Potential*

The chemical potential enters in the continuum QCD partition function as

$$i\gamma_0 A_0 \rightarrow i\gamma_0 A_0 + \mu\gamma_0. \quad (142)$$

resulting in the chRMT Dirac operator<sup>54</sup>

$$D(\mu) = \begin{pmatrix} 0 & iW + \mu \\ iW^\dagger + \mu & 0 \end{pmatrix}. \quad (143)$$

If we notice that  $\mu\gamma_0$  has the same reality properties as  $\gamma_0\partial_0$ , we immediately conclude<sup>155</sup> that these ensembles can be classified according to the same anti-unitary symmetries as the chRMT's for  $\mu = 0$ . However, the term proportional to  $\mu$  violates the anti-Hermiticity of the Dirac operator, and typically the eigenvalues of  $D(\mu)$  will be scattered in the complex plane.

Many of the problems associated with the presence of a chemical potential are related to the loss of non-Hermiticity. Exactly, these problems are reproduced by the chRMT partition function with Dirac operator given by (143). For example, in this model one can study the problems of the quenched approximation<sup>142,143,144</sup>, the structure of the Yang-Lee zeros<sup>145,57</sup> and the problems with the Glasgow method<sup>146</sup>. Below we will discuss the first two applications.

#### 7.5 *Yang-Lee Zeros*

The QCD partition function

$$Z(m, \mu) = \int \det^{N_f}(D + m + \mu\gamma_0) e^{-S_{YM}} \quad (144)$$

is a polynomial in  $m$  and  $\mu$ . For simplicity, let us consider the case  $m = 0$ . Then<sup>147</sup>

$$Z^{QCD}(m = 0, \mu) \sim \prod_k (\mu - \mu_k), \quad (145)$$

and the baryon density is given by

$$n_B = \frac{1}{V} \partial_\mu \log Z(m=0, \mu) = \frac{1}{V} \sum_k \frac{1}{\mu - \mu_k}. \quad (146)$$

With the zeros scattered in the complex  $\mu$ -plane we can interpret the real and imaginary parts of  $n_B$  as the electric field at  $\mu$  due to charges located at  $\mu_k$ .

Physically, we expect that  $n_B = 0$  for  $\mu < \mu_c \neq 0$  and jumps to a finite value at  $\mu = \mu_c$ . We thus expect a first order phase transition at  $\mu_c$ . Two possibilities for the distribution of the zeros come to mind. First, according to Gauss law, a homogenous distribution of zeros  $\mu_k$  along the complex circle  $|\mu| = \mu_c$  results in a zero baryon number density for  $|\mu| < \mu_c$ . (Of course in the thermodynamic limit, a subleading number of zeros may be present inside the circle.). Second, we all know that the electric field is zero between two infinite parallel plates with equal constant charge density is zero. The analogue of this phenomenon in two dimensions is that the electric field is zero between two parallel infinite line charges with constant charge density. Therefore, the second possibility is that the zeros in the complex  $\mu$ -plane are located at

$$\mu_k = \pm \mu_c + \frac{k\pi i}{2\beta}, \quad k \text{ odd}. \quad (147)$$

We also expect that the baryon number density increases smoothly for  $\mu > \mu_c$ . This requires a radially symmetric cloud of zeros outside of the radius  $|\mu| = \mu_c$  in the first case, and a constant density parallel to the imaginary axis for  $|\text{Re}(\mu)| > \mu_c$  in the second case.

The simplest possible model for spherically symmetric distributed zeros of the partition function, is one with zeros given by the roots of unity,

$$\mu_k = \mu_c e^{\frac{2\pi i k}{N}}, \quad k = 1, \dots, N. \quad (148)$$

This results in the partition function

$$Z(\mu) = \prod_k (\mu - \mu_k) = \mu^N - \mu_c^N. \quad (149)$$

For the baryon number density we then obtain

$$\begin{aligned} n_B &= \frac{1}{N} \partial_\mu \log Z = \frac{\mu^{N-1}}{\mu^N - \mu_c^N} \\ &= \begin{cases} \frac{1}{\mu} & \text{for } |\mu| > \mu_c \\ 0 & \text{for } |\mu| < \mu_c \end{cases} \quad \text{for } N \rightarrow \infty. \end{aligned} \quad (150)$$

In the second case with zeros given by (147), the partition function is given by

$$Z(\mu) = \prod_{k \text{ odd}} (\mu - \mu_c - \frac{k\pi i}{2\beta})(\mu + \mu_c - \frac{k\pi i}{2\beta}). \quad (151)$$

Up to a constant the zeros are given by the zeros of the cosh-function. We thus find that

$$\frac{Z(\mu)}{Z(0)} = \frac{\cosh(\beta(\mu_c - \mu)) \cosh(\beta(\mu_c + \mu))}{\cosh^2(\mu_c)}. \quad (152)$$

The baryon density is then given by (in an arbitrary normalization)

$$n_B = \frac{1}{2\beta} \partial_\mu \log Z(\mu) = \frac{\sinh(2\beta\mu)}{\cosh(2\beta\mu) + \cosh(2\beta\mu_c)}. \quad (153)$$

For  $\beta \rightarrow \infty$  this can be approximated by

$$n_B = \frac{1}{1 + e^{2\beta(\mu_c - \mu)}}, \quad (154)$$

and we find that

$$n_B = 0 \quad \text{for} \quad \mu < \mu_c, \quad (155)$$

$$n_B = 1 \quad \text{for} \quad \mu > \mu_c. \quad (156)$$

In the next section we will study the baryon number density in the chiral random matrix model at nonzero chemical potential.

### 7.6 Phases in chRMT at $\mu \neq 0$

The chRMT partition function at  $\mu \neq 0$  is obtained from the finite  $T$  partition function by the replacement  $T \rightarrow i\mu$ . For  $N_f = 1$  this results in the  $\sigma$  model

$$Z(\mu) = \int d\sigma d\sigma^* (|\sigma|^2 - \mu^2)^N e^{-N|\sigma|^2}. \quad (157)$$

For  $N \rightarrow \infty$ , the integrals in this partition function can be performed by a saddle point approximation. We find that

$$\bar{\sigma} = 0 \quad \text{for} \quad \mu > \mu_c \Rightarrow Z = \mu^{2N}, \quad (158)$$

$$\bar{\sigma} = \sqrt{1 + \mu^2} \quad \text{for} \quad \mu < \mu_c \Rightarrow Z = e^{-N(\mu^2 + 1)}. \quad (159)$$

The critical point is given by the transcendental equation<sup>54</sup>  $\mu_c^2 = \exp(-1 - \mu_c^2)$  which is solved by  $\mu_c \approx 0.53$

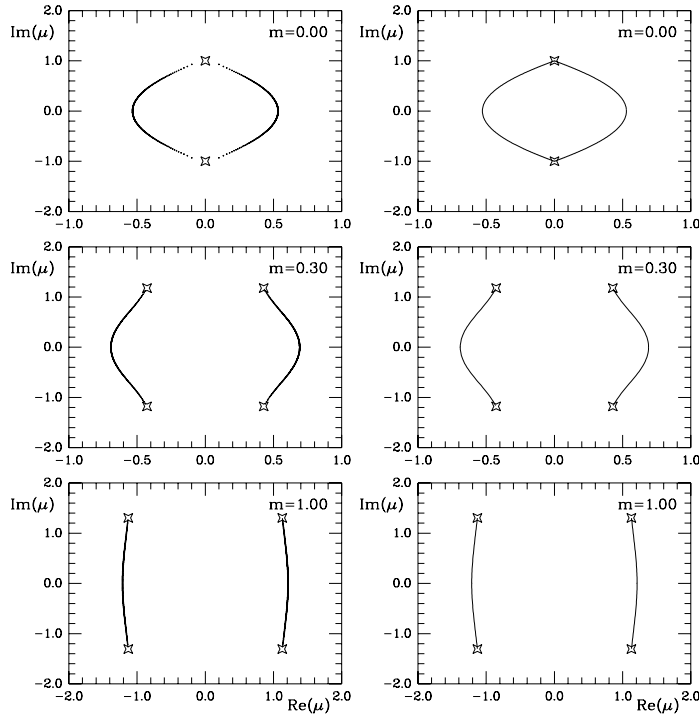


Figure 5: The zeros of the partition function in the complex  $\mu$  plane (left) and the result obtained from a mean field analysis (right). Results are given for  $m = 0$  (upper),  $m = 0.30$  (middle), and  $m = 1.0$  (lower) for  $N = 192$ . The zeros of the discriminant of the cubic equation are denoted by stars. Note that the scale on the  $x$ -axis of the lower figure is different.

We find that the baryon number density above the critical point shows the same behavior as in our naive model. However, the baryon density for  $\mu < \mu_c$  is nonvanishing which disagrees with our expectation for QCD at zero temperature and finite density. The remedy should be clear. In order to obtain a sharp Fermi-Dirac distribution one has to sum over all Matsubara frequencies<sup>148</sup>. This point was ignored in our model. In the next section we discuss a RMT  $\sigma$ -model that explicitly includes the lowest two Matsubara frequencies. This model can be trivially extended to include all Matsubara frequencies, and the infinite product can be evaluated analytically in terms of a cosh-function. For  $\beta \rightarrow \infty$  we find<sup>56</sup> that the zeros of the partition function in the complex

$\mu$ -plane are located on the line  $\text{Re}(\mu) = \pm\mu_c$ .

A much more disturbing observation is that in the thermodynamic limit the partition function for  $\mu < \mu_c$  becomes exponentially small<sup>57,30</sup>. This exponential cancellation is due to the phase of the eigenvalues. It makes accurate numerical simulations forbiddingly difficult.

The random matrix partition function is a polynomial in  $m$  and  $\mu$  and it is straightforward to study the zeros of the partition function in the complex  $m$ -plane or the complex  $\mu$ -plane. To assure our numerical accuracy we have determined the zeros of the polynomials by means of multi-precision algorithms<sup>149</sup> using as much as 1000 significant digits. The results are shown in Fig. 5. The branch points at the end of a cut are the points where two saddle-point solutions coincide. In the present case they are given by zeros of the discriminant of a cubic equation. The line of zeros can also be obtained from a saddle point analysis (see right half of the figure). For more details and results in other fields<sup>150,151</sup> we refer to the original literature.

### 7.7 Failure of the Quenched Approximation

For QCD with three or more colors and fermions in the fundamental representation, the fermion determinant is complex. The presence of this phase makes Monte-Carlo simulations impossible. A way out might be the quenched approximation, i.e. ignore the fermion determinant altogether and hope that it will work. This approach was followed in<sup>142,143</sup> with the conclusion that the critical chemical potential is given by the pion mass instead of the nucleon mass. Obviously, this result is physically wrong!

This problem was first analyzed in chRMT by Stephanov<sup>54</sup>. He showed that the quenched limit is the limit  $N_f \rightarrow 0$  of a partition functions with fermion determinant

$$|\det(D(\mu) + m)|^{N_f} \quad (160)$$

rather than

$$(\det(D(\mu) + m))^{N_f}. \quad (161)$$

The absolute value can be represented as (let us take  $N_f = 2$  for simplicity)

$$\det(D(\mu) + m) \det(D^\dagger(\mu) + m^*) = \int D\psi D\psi^c e^{\bar{\psi}(D(\mu)+m)\psi + \bar{\psi}^c(D^\dagger(\mu)+m^*)\psi^c}, \quad (162)$$

and Goldstone bosons made out of quarks and conjugate anti-quarks carry a net baryon number resulting in a critical chemical potential given by the pion mass.

The random matrix model corresponding to (162) can be mapped onto a nonlinear  $\sigma$ -model which can be solved by a saddle-point approximation. The exact solution of this model confirms that the critical chemical potential is proportional to  $\sqrt{m}$ , the same dependence as for the pion mass.

### 7.8 The Chiral Phase Transition in chRMT

In previous section we have studied a model at nonzero temperature and a model at nonzero chemical potential. These two models can be combined in the following schematic chRMT model<sup>58</sup> for the chiral phase transition,

$$Z = \int DW \det^{N_f} \begin{pmatrix} m & iW + iC \\ iW^\dagger + iC & im \end{pmatrix} \quad (163)$$

with  $C$  a diagonal matrix with  $C_k = a\pi T - ib\mu$  for one half of the diagonal elements and  $C_k = -a\pi T - ib\mu$  for the other half with  $a$  and  $b$  dimensionless parameters. This model can be considered as the matrix equivalent of a Landau-Ginzburg functional. We thus expect to find mean field critical exponents. The advantage over using Landau-Ginzburg theory is that in this case the spectrum of the Dirac operator is accessible. In particular, this might reveal interesting behavior of the Dirac spectrum near the critical point. For example, for  $\mu = 0$  we have shown that the fluctuations of the smallest eigenvalue of the Dirac operator can be used as an order parameter for the chiral phase transition<sup>51</sup>.

Also in this case the partition function can be reduced to a  $\sigma$ -model, For the simplest case of  $N_f = 1$  it is given by

$$Z(T, \mu) = \int d\sigma e^{-N\Omega(\sigma)}, \quad (164)$$

where

$$\begin{aligned} \Omega(\sigma) = & \sigma\sigma^\dagger - \log((\sigma + m)(\sigma^\dagger + m) - (\mu + iT)^2) \\ & - \log((\sigma + m)(\sigma^\dagger + m) - (\mu - iT)^2). \end{aligned} \quad (165)$$

The chiral condensate is given by the expectation value of  $\sigma$ . The saddle-point equation is a fifth order equation in  $\sigma$ . Therefore this model is very similar to a  $\phi^6$  Landau-Ginzburg theory. For  $m = 0$  we find that  $\sigma$  is real and the saddle

point-equation is given by

$$\sigma[\sigma^4 - 2(\mu^2 - T^2 + \frac{1}{2})\sigma^2 + (\mu^2 + T^2)^2 + \mu^2 - T^2] = 0. \quad (166)$$

The critical points occur where one of the solutions of the cubic equation merge with the solution  $\sigma = 0$ , i.e. along the curve  $(\mu^2 + T^2)^2 + \mu^2 - T^2 = 0$ . At the tri-critical point three solution merge. This happens if in addition  $\mu^2 - T^2 + \frac{1}{2} = 0$ .

In Fig. 6 we show the phase diagram in the  $\mu T m$  space. In the  $m = 0$  plane we observe a line of second order phase transitions and a line of first order phase transitions. They join at the tricritical point. Also joining at the tricritical point is a line of second order phase transitions in the  $m$ -directions which is the boundary of the plane of first order transitions in  $\mu T m$ -space.

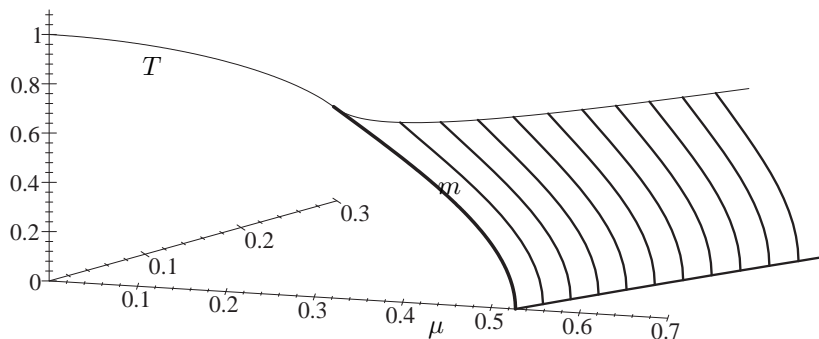


Figure 6: Phase diagram of QCD with two light flavors of mass  $m$  as calculated from the random matrix model. The almost parallel curves on the wing surface are cross sections of this surface with  $m = \text{const}$  planes.

### 7.9 Possibility of a Localization Transition in QCD

From the theory of Anderson localization we know that the eigenvalues corresponding to localized states are statistically independent and thus obey Poisson statistics. Since it has been well established that in QCD at zero temperature the correlations of the eigenvalues of the QCD Dirac operator are given by chiral Random Matrix theory, we conclude that the eigenstates are extended. This also follows from a direct analysis of the Dirac wave functions for gauge field configurations given by a liquid of instantons. However, we wish to point



out that studies with Wilson Dirac fermions indicate that eigenfunctions are localized<sup>161</sup>. We do not have an explanation for this discrepancy.

One reason to expect a localization transition with increasing temperature is dimensional reduction. States are more likely to be localized in lower dimensions. For example, in a one-dimensional disordered system all states are localized. On the other hand, because of asymptotic freedom the coupling becomes weaker at higher temperatures. Let us analyze more closely what will happen.

Lattice simulations for the valence quark mass dependence of the chiral condensate were performed for temperatures both below and above the critical temperature<sup>76</sup>. It was found that, in the ergodic domain, all data can be rescaled onto a universal curve given by chRMT. This shows that the states are extended below the critical point.

According to a theoretical argument due to Parisi<sup>162</sup> given in the context of disordered systems a localization transition can only occur in quenched theories. In QCD, this argument can be translated as follows. Let us assume that the eigenfunctions of the Dirac operator are localized. Then the joint eigenvalue distribution factorizes in one-particle distributions  $(\lambda^2 + m^2)^{N_f} F(\lambda)$ . The average spectral density is thus given by

$$\begin{aligned} \rho(\lambda_1) &= \int d\lambda_2 \cdots d\lambda_n \prod_{k=1}^n (\lambda_k^2 + m^2)^{N_f} F(\lambda_1) \cdots F(\lambda_n) \\ &= c_1 (\lambda_1^2 + m^2)^{N_f} F(\lambda_1). \end{aligned} \quad (167)$$

We then find

$$\lim_{\lambda_1 \rightarrow 0} \lim_{m \rightarrow 0} \lim_{V \rightarrow \infty} \rho(\lambda_1) = 0, \quad (168)$$

i.e., no spontaneous breaking of chiral symmetry. We thus conclude that in the chiral limit no localization can occur in QCD with light quarks. What happens in quenched theories remains an open question. However, studies with long range interactions given by  $\sim \pm 1/|R_i - R_j|^d$  with random signs and random positions  $R_i$  as is the case for instanton liquid simulations indicate that all states are delocalized<sup>152</sup>.

### 7.10 Triality at $\mu \neq 0$

Let us finally discuss how Dirac spectra at nonzero chemical potential depend on the Dyson index of the matrix elements. We remind the reader that the classification of Dirac operators with chemical potential is the same as for zero chemical potential.

Numerical simulations have been performed for all three classes. A cut along the imaginary axis below a cloud of eigenvalues was found in instanton liquid simulations<sup>153</sup> for  $N_c = 2$  at  $\mu \neq 0$  which corresponds to  $\beta = 1$ . In lattice QCD simulations with staggered fermions for  $N_c = 2$ <sup>154</sup> a depletion of eigenvalues along the imaginary axis was observed, whereas for  $N_c = 3$  the eigenvalue distribution did not show any pronounced features<sup>142</sup>.

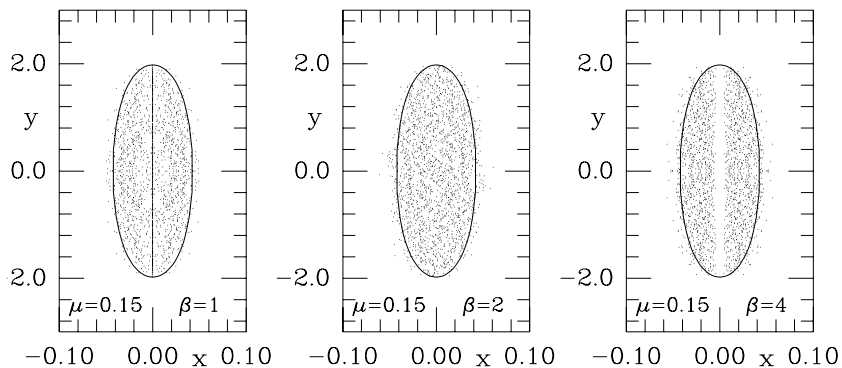


Figure 7: Scatter plot of the real ( $x$ ), and the imaginary parts ( $y$ ) of the eigenvalues of the random matrix Dirac operator at nonzero chemical potential. The values of  $\beta$  and  $\mu$  are given in the labels of the figure. The full curve shows the analytical result for the boundary.

In the quenched approximation, the spectral properties of the random matrix Dirac operator (143) can easily be studied numerically by diagonalizing a set of matrices with probability distribution (106). In Fig. 7 we show results<sup>155</sup> for the eigenvalues of a few  $100 \times 100$  matrices for  $\mu = 0.15$  (dots). The solid curve represents the analytical result for the boundary of the domain of eigenvalues derived in<sup>54</sup> for  $\beta = 2$ . However, the method that was used can be extended<sup>155</sup> to  $\beta = 1$  and  $\beta = 4$  and with the proper scale factors we find exactly the same solution.

For  $\beta = 1$  and  $\beta = 4$  we observe exactly the same structure as in the previously mentioned (quenched) QCD simulations. We find an accumulation of eigenvalues on the imaginary axis for  $\beta = 1$  and a depletion of eigenvalues along this axis for  $\beta = 4$ . This depletion can be understood as follows. For  $\mu = 0$  all eigenvalues are doubly degenerate. This degeneracy is broken at  $\mu \neq 0$  which produces the observed repulsion between the eigenvalues.

The number of purely imaginary eigenvalues for  $\beta = 1$  scales as  $\sqrt{N}$  and is thus not visible in a leading order saddle point analysis. Such a  $\sqrt{N}$  scaling is typical for the regime of weak non-hermiticity first identified by Fyodorov *et al.*<sup>157</sup>. Using the supersymmetric method of random matrix theory the  $\sqrt{N}$

dependence was obtained analytically by Efetov<sup>158</sup>. Also the case  $\beta = 4$  was analyzed analytically in<sup>159</sup> with results that are in complete agreement with our numerical simulations. Obviously, more work has to be done in order to arrive at a complete characterization of universal features<sup>160</sup> in the spectrum of nonhermitean matrices.

## 8 Closing Remarks

In these lectures we have presented analytical results for the infrared limit of the QCD Dirac spectrum. We have shown that the correlations of the Dirac eigenvalues for level spacings below the Thouless energy are given by the zero momentum limit of the partially quenched chiral partition function and agree with results obtained from chiral random matrix theory. A key ingredient in the formulation of the effective theory is the structure of the integration manifold. We have argued that it is given by a super-Riemannian manifold which is characterized by a symbiosis between compact and noncompact degrees of freedom. We have shown that the valence quark mass dependence of the chiral condensate that follows from the zero momentum sector of the effective chiral partition function coincides with the result from chiral Random Matrix Theory. In this formulation, universality is natural. The structure of the chiral Lagrangian only depends on the pattern of chiral symmetry breaking.

An important condition for the validity of the chiral Lagrangian is the requirement that the only low-lying modes are the Goldstone modes associated with the spontaneous breaking of chiral symmetry. Without confinement this would not be the case. On the other hand, according to the Bohigas conjecture, eigenvalue correlations are given by random matrix theory if the corresponding classical system is chaotic. If the classical motion of quarks in 4+1 dimensions is chaotic the eigenvalues of the Dirac operator are correlated according to chRMT. Then necessarily the low-energy dynamics is given by the chiral Lagrangian and this can only happen if we have confinement.

Can we reverse this statement? Is the classical motion of a fermion in a confining theory necessarily chaotic? The point I wish to make is that the Bohigas conjecture and confinement are not unrelated. For a deeper understanding of confinement a proof of the Bohigas conjecture might be required. Recent progress in this direction is encouraging<sup>163,164,165,166,167</sup>.

## 9 Acknowledgments

I wish to thank the organizers of the Osaka school and the Kyoto workshop for their hospitality and for organizing such a wonderful meeting. In writing this review I have benefitted greatly from discussions and collaborations with

Gernot Akemann, Igor Aleiner, Alexander Altland, Poul Damgaard, Yan Fyodorov, Meinulf Göckeler Thomas Guhr, Adam Halasz, Bertram Klein, Andy Jackson, Steffen Meyer, Shinsuke Nishigaki, James Osborn, Paul Rakow, Andreas Schäfer, Melih Sener, Ben Simons, Robert Shrock, Edward Shuryak, Andrei Smilga, Misha Stephanov, Dominique Toublan, Hans Weidenmüller, Tilo Wettig and Martin Zirnbauer. Dominique Toublan is acknowledged for a critical reading of the manuscript.

## References

1. C. DeTar, *Quark-gluon plasma in numerical simulations of QCD*, in *Quark gluon plasma 2*, R. Hwa ed., World Scientific 1995.
2. A. Ukawa, Nucl. Phys. Proc. Suppl. **53** (1997) 106.
3. A. Smilga, Phys. Rep. **291** (1997) 1.
4. F.Karsch, Nucl. Phys. Proc. Suppl. **60A** (1998) 169.
5. T. Banks and A. Casher, Nucl. Phys. **B169** (1980) 103.
6. O. Bohigas, M. Giannoni, Lecture notes in Physics **209** (1984) 1; O. Bohigas, M. Giannoni and C. Schmit, Phys. Rev. Lett. **52** (1984) 1.
7. T. Guhr, A. Müller-Groeling and H.A. Weidenmüller, Phys. Rep. **299** (1998) 189.
8. H. Leutwyler and A. Smilga, Phys. Rev. **D46** (1992) 5607.
9. L. Schäfer and F. Wegner, Z. Phys. **B38** (1980) 113.
10. A.J. McKane and M. Stone, Ann. Phys. (NY) **131** (1981) 36.
11. K. Efetov, Adv. Phys. **32**, 53 (1983).
12. J.J.M. Verbaarschot, H.A. Weidenmüller, and M.R. Zirnbauer, Phys. Rep. **129**, 367 (1985).
13. J.J.M. Verbaarschot in *Continuous Advances in QCD*, A.V. Smilga ed., p. 195, World Scientific, 1994 ( hep-th/9405006).
14. J.C. Osborn and J.J.M. Verbaarschot, Phys. Rev. Lett. **81** (1998) 268.
15. J.C. Osborn and J.J.M. Verbaarschot, Nucl. Phys. **B525** (1998) 738.
16. J. Osborn, D. Toublan and J. Verbaarschot, Nucl. Phys. **B** (in press) hep-th/9806110.
17. P. Damgaard, J. Osborn, D. Toublan and J. Verbaarschot, hep-th/9811212, Nucl. Phys. **B** (in press).
18. A. Morel, J. Physique **48** (1987) 1111.
19. C. Bernard and M. Golterman, Phys. Rev. D49 (1994) 486; C. Bernard and M. Golterman, hep-lat/9311070.
20. S. Sharpe, Phys. Rev. D 56 (1997) 7052.
21. J. Gasser and H. Leutwyler, Phys. Lett. **188B** (1987) 477.
22. J.J.M. Verbaarschot, Phys. Lett. **B368** (1996) 137.

23. J.J.M. Verbaarschot, in *Nonperturbative Approaches to Quantum Chromodynamics*, D. Diakonov, ed., Gatchina 1995.
24. E.V. Shuryak and J.J.M. Verbaarschot, Nucl. Phys. **A560** (1993) 306.
25. J.J.M. Verbaarschot, Phys. Rev. Lett. **72** (1994) 2531; Phys. Lett. **B329** (1994) 351.
26. C.W.J. Beenakker, Rev. Mod. Phys. **69** (1997) 731.
27. G. Montambaux, in *Quantum Fluctuations, Les Houches, Session LXIII*, E. Giacobino, S. Reynaud and J. Zinn-Justin, eds., Elsevier Science, 1995, cond-mat/9602071.
28. B.L. Altshuler, I.Kh. Zharekeshev, S.A. Kotochigova and B.I. Shklovskii, Zh. Eksp. Teor. Fiz. **94** (1988) 343.
29. E. Shuryak, Nucl. Phys. **B302** (1988) 599; D. Diakonov, *Talk given at International School of Physics, 'Enrico Fermi', Course 80: Selected Topics in Nonperturbative QCD*, Varenna, 1995, hep-ph/9602375.
30. M.A. Halasz and J.J.M. Verbaarschot, Phys. Rev. Lett. **74** (1995) 3920; M.A. Halasz, T. Kalkreuter and J.J.M. Verbaarschot, Nucl. Phys. Proc. Suppl. **53** (1997) 266.
31. M.E. Berbenni-Bitsch, S. Meyer, A. Schäfer, J.J.M. Verbaarschot and T. Wettig, Phys. Rev. Lett. **80** (1998) 1146.
32. J.Z. Ma, T. Guhr and T. Wettig, Eur. Phys. J. **A2** (1998) 87.
33. M.E. Berbenni-Bitsch, A.D. Jackson, S. Meyer, A. Schafer, J.J.M. Verbaarschot and T. Wettig, Nucl. Phys. Proc. Suppl. **63** (1998) 820.
34. M.E. Berbenni-Bitsch, M. Gockeler, T. Guhr, A.D. Jackson, J.Z. Ma, S. Meyer, A. Schäfer, H.A. Weidenmüller, T. Wettig and T. Wilke, Phys. Lett. **B438** (1998) 14.
35. T. Guhr, J.Z. Ma, S. Meyer and T. Wilke, *Statistical analysis and the equivalent of a Thouless energy in lattice QCD Dirac spectra*, hep-lat/9806003.
36. M.E. Berbenni-Bitsch, S. Meyer and T. Wettig, Phys. Rev. **D58** (1998) 071502.
37. H. Markum, R. Pullirsch, K. Rabitsch and T. Wettig, Nucl. Phys. Proc. Suppl. **63** (1998) 832.
38. R. Pullirsch, H. Markum, K. Rabitsch and T. Wettig, hep-lat/9809057.
39. R. Pullirsch, K. Rabitsch, T. Wettig and H. Markum, Phys. Lett. **B427** (1998) 119.
40. P.H. Damgaard, U.M. Heller, A. Krasnitz and T. Madsen, Phys. Lett. **B440** (1998) 129.
41. P.H. Damgaard, U.M. Heller and A. Krasnitz, hep-lat/981006.
42. M. Gockeler, H. Hehl, P.E.L. Rakow, A. Schafer and T. Wettig, Phys. Rev. **D** (in press) hep-lat/9811018.

43. R.G. Edwards, U.M. Heller and R. Narayanan, hep-lat/9902021. Authors: Robert G. Edwards, Urs M. Heller and Rajamani Narayanan
44. R.G. Edwards, U.M. Heller, J. Kiskis and R. Narayanan, hep-th/9902117.
45. B.A. Berg, H. Markum, R. Pullirsch, hep-lat/9812010.
46. R. Janik, M. Nowak, G. Papp and I. Zahed, Phys. Lett. **B389** (1996) 341.
47. H. Hehl and A. Schafer, hep-ph/9806372.
48. M.E. Berbenni-Bitsch, M. Gockeler, H. Hehl, S. Meyer, P.E.L. Rakow, A. Schäfer and T. Wettig, hep-lat/9901013.
49. J.J.M. Verbaarschot, Nucl. Phys. **B427** (1994) 534.
50. M.F.L. Golterman and K.C. Leung, hep-lat/9711033; M.F.L. Golterman, Acta Phys. Polon. **B25** (1994).
51. A.D. Jackson and J.J.M. Verbaarschot, Phys. Rev. **D53** (1996) 7223.
52. T. Wettig, A. Schäfer and H. Weidenmüller, Phys. Lett. **B367** (1996) 28.
53. M. Stephanov, Phys. Lett. **B275** (1996) 249; Nucl. Phys. Proc. Suppl. **53** (1997) 469.
54. M. Stephanov, Phys. Rev. Lett. **76** (1996) 4472.
55. R. Janik, M. Nowak, G. Papp and I. Zahed, Acta Phys. Polon. **B28** (1997) 2949. hep-ph/9708418; R. Janik, M.A. Nowak, G. Papp, J. Wambach, and I. Zahed, Phys. Rev. **E55** (1997) 4100; R. Janik, M.A. Nowak, G. Papp and I. Zahed, Nucl. Phys. B501 (1997) 603.
56. J.J.M. Verbaarschot, in preparation.
57. M.A. Halasz, A.D. Jackson and J.J.M. Verbaarschot, Phys. Lett. **B395** (1997) 293; Phys. Rev. **D56** (1997) 5140.
58. M. Halasz, A. Jackson, R. Shrock, M. Stephanov and J. Verbaarschot, Phys. Rev. **D58** (1998) 096007.
59. J. Feinberg and A. Zee, Nucl. Phys. **B504** (1997) 579; Nucl. Phys. **B501** (1997) 643.
60. T. Blum, this volume.
61. C. Vafa and E. Witten, Nucl. Phys. **B234** (1984) 173.
62. M. Peskin, Nucl. Phys. **B175** (1980) 197; S. Dimopoulos, Nucl. Phys. **B168** (1980) 69; M. Vysotskii, Y. Kogan and M. Shifman, Sov. J. Nucl. Phys. **42** (1985) 318; D.I. Diakonov and V.Yu. Petrov, Lecture notes in physics, **417**, Springer 1993.
63. J. Stern, we thank him for raising this point.
64. D.I. Diakonov and V. Yu. Petrov, Nucl. Phys. **B272** (1986) 457.
65. H.B. Nielsen and M. Ninomiya, Nucl. Phys. **185** (1981) 20.
66. W. Bardeen, A. Duncan, E. Eichten, G. Hockney and H. Thacker, Phys. Rev. **D57** (1998) 1633. and H. Thacker, *Quenched approximation arti-*

- facts: a detailed study in two-dimensional QED*, hep-lat/9705002.
67. C.R. Gattringer, I. Hip and C.B. Lang, Nucl. Phys. **B508** (1997) 329.
  68. C. Gattringer, I. Hip and C. Lang, Nucl. Phys. **B508** (1997) 329.
  69. C. Gattringer and I. Hip, Nucl. Phys. **B536** (1998) 363.
  70. F. Farchioni, I. Hip, C.B. Lang, M. Wohlgenannt, hep-lat/9812018.
  71. J. Negele, hep-lat/9810053.
  72. R. Narayanan, hep-lat/9810045,
  73. S. Hands and M. Teper, Nucl. Phys. **B347** (1990) 819.
  74. J.B. Kogut, J.-F. Lagae and D.K. Sinclair, Nucl. Phys. Proc. Suppl. **63** (1998) 433.
  75. T. Schäfer and E. Shuryak, Rev. Mod. Phys. **70** (1998) 323.
  76. S. Chandrasekharan, Nucl. Phys. Proc. Suppl. **42** (1995) 475; S. Chandrasekharan and N. Christ, Nucl. Phys. Proc. Suppl. **42** (1996) 527; N. Christ, Lattice 1996.
  77. A.V. Andreev, B.D. Simons, and N. Taniguchi, Nucl. Phys **B432** [FS] (1994) 487.
  78. A.D. Jackson, M.K. Sener and J.J.M. Verbaarschot, Nucl. Phys. **B479** (1996) 707.
  79. T. Guhr and T. Wettig, Nucl. Phys. **B506** (1997) 589.
  80. A.D. Jackson, M.K. Sener and J.J.M. Verbaarschot, Nucl. Phys. **B506** (1997) 612.
  81. J. Gasser and H. Leutwyler, Ann. Phys. **158**, 142 (1984); J. Gasser and H. Leutwyler, Nucl. Phys. **B250**, 465 (1985).
  82. H. Leutwyler, Ann. Phys. **235** (1994) 165.
  83. M. Zirnbauer, J. Math. Phys. **37** (1996) 4986.
  84. F.A. Berezin, *Introduction to superanalysis*, Reidel, Dordrecht (1987).
  85. K.B. Efetov, *Supersymmetry in disorder and chaos*, Cambridge University Press, (1997); K.B. Efetov, Adv. Phys. **32** (1983) 53.
  86. B. Simons and A. Altland, cond-mat/9811134.
  87. M.R. Zirnbauer, J. Math. Phys. **38** (1997) 2007; J. Phys. **A 29** (1996) 7113.
  88. H.A. Weidenmüller, Nucl. Phys. A 518 (1990) 1.
  89. T. Guhr and A. Mueller-Groeling, cond-mat/9702113, J. Math. Phys. (in press).
  90. N. Argaman, Y. Imry and U. Smilansky, Phys. Rev. **B47** (1993) 4440.
  91. V.E. Kravtsov, in *Correlated Fermions and Transport in Mesoscopic Systems*, Les Arcs, 1996, cond/mat9603166.
  92. A. Altland and Y. Gefen, Phys. Rev. Lett. **71** (1993) 3339.
  93. D. Braun and G. Montambaux, Phys. Rev. **52** (1995) 13903.
  94. A.G. Aronov and A.D. Mirlin, Phys. Rev. **B51** (1995) 6131.

95. Y.V. Fyodorov and A.D. Mirlin, Phys. Rev. **B51** (1995) 13403.
96. V.E. Kravtsov, I.V. Lerner, B.L. Altshuler and A.G. Aronov, Phys. Rev. Lett. **72** (1994) 888.
97. A. Altland, Y. Gefen and G. Montambaux, Phys. Rev. Lett. **76** (1996) 1130.
98. J.T. Chalker, V.E. Kravtsov, I.V. Lerner, JETP Lett. **64** (1996) 386.
99. R. Janik, M.A. Nowak, G. Papp and I. Zahed, Phys. Rev. Lett. **81** (1998) 264.
100. R. Brower, P. Rossi and C-I. Tan, Nucl.Phys. **B190** [FS3] (1981) 699; R. Brower and M. Nauenberg, **B180** [FS2] (1981) 221.
101. P. Hasenfratz and H. Leutwyler, Nucl. Phys. **B343** (1990) 241.
102. P.H. Damgaard, Phys. Lett. **B425** (1998) 151.
103. A. Smilga and J. Stern, Phys. Lett. **B318** (1993) 531.
104. J.J.M. Verbaarschot and I. Zahed, Phys. Rev. Lett. **70** (1993) 3852.
105. A. Altland, M.R. Zirnbauer, Phys. Rev. Lett. **76** (1996) 3420.
106. A. Smilga and J.J.M. Verbaarschot, Phys. Rev. **D51** (1995) 829.
107. J.J.M. Verbaarschot, *Lectures given at NATO Advanced Study Institute on Confinement, Duality and Nonperturbative Aspects of QCD*, Cambridge, 1997, hep-th/9710114.
108. T. Akuzawa and M. Wadati, J. Phys. Soc. Jap. **67** (1998) 2151.
109. K. Slevin and T. Nagao, Phys. Rev. Lett. **70** (1993) 635.
110. D. Fox and P. Kahn, Phys. Rev. **134** (1964) B1152; (1965) 228.
111. T. Nagao and M. Wadati, J. Phys. Soc. Japan **60** (1991) 2998; J. Phys. Soc. Jap. **60** (1991) 3298; J. Phys. Soc. Jap. **61** (1992) 78; J. Phys. Soc. Jap. **61** (1992) 1910. **61** (1992) 78, 1910.
112. P. Forrester, Nucl. Phys. **B[FS]402** (1993) 709.
113. S.M. Nishigaki, P.H. Damgaard and T. Wettig, hep-th/9803007.
114. P.H. Damgaard and S.M. Nishigaki, Nucl. Phys. **B518** (1998) 495.
115. T. Wilke, T. Guhr and T. Wettig, Phys. Rev. **D57** (1998) 6486; B. Seif, T. Wettig and T. Guhr, hep-th/9811044.
116. J. Jurkiewicz, M. Nowak and I. Zahed, Nucl. Phys. **B478** (1996) 605; Erratum-ibid. **B513** (1998) 759.
117. M.J. Bowick and E. Brézin, Phys. Lett. **B 268**, 21 (1991).
118. G. Hackenbroich and H.A. Weidenmüller, Phys. Rev. Lett. **74** (1995) 4118.
119. E. Brézin, S. Hikami and A. Zee, Nucl. Phys. **B464** (1996) 411.
120. G. Akemann, P. Damgaard, U. Magnea and S. Nishigaki, Nucl. Phys. **B 487[FS]** (1997) 721.
121. E. Kanzieper and V. Freilikher, Phys. Rev. Lett. **78**, 3806 (1997); Phys. Rev. **E 55**, 3712 (1997).



122. V. Freilikher, E. Kanzieper and I. Yurkevich, Phys. Rev. **E53**, 2200 (1996).
123. P. Zinn-Justin, Nucl. Phys. **B497** (1997) 725.
124. B. Eynard, Nucl. Phys. **B506**, 633 (1997).
125. E. Brézin and S. Hikami, Phys. Rev. **E56**, 264 (1997).
126. C.W.J. Beenakker, Phys. Rev. Lett. **70**, 1155 (1993).
127. J.J.M. Verbaarschot, Nucl. Phys. **B426** (1994) 559.
128. M.K. Sener and J.J.M. Verbaarschot, hep-th/9801042.
129. H. Widom, solv-int/9804005.
130. P.H. Damgaard, S.M. Nishigaki, Phys. Rev. **D57** (1998) 5299.
131. J. Christiansen, hep-th/9809194.
132. K. Splittorff and A.D. Jackson, hep-lat/9805018. K. Splittorff, hep-th/9810248.
133. P.H. Damgaard, Phys. Lett. **B424** (1998) 322; G. Akemann and P.H. Damgaard, Phys. Lett. **B432** (1998) 390/ G. Akemann and P.H. Damgaard, Nucl. Phys. **B528** (1998) 411.
134. F. Dyson and M. Mehta, J. Math. Phys. **4** (1963) 701.
135. M. Mehta, *Random Matrices*, Academic Press, San Diego 1991.
136. T. Kalkreuter, Phys. Lett. **B276** (1992) 485; Phys. Rev. **D48** (1993) 1; Comp. Phys. Comm. **95** (1996) 1.
137. J. Cullum and R.A. Willoughby, J. Comp. Phys. **44** (1981) 329.
138. A. Pandey, Ann. Phys. **134** (1981) 119.
139. T. Nagao and P.J. Forrester, Nucl. Phys. **B435** (1995) 401.
140. P.W. Anderson, Phys. Rev. **109** (1958) 1492.
141. P. Di Francesco, P. Ginsparg, and J. Zinn-Justin, Phys. Rep. **254** (1995) 1.
142. I. Barbour, N. Behihil, E. Dagotto, F. Karsch, A. Moreo, M. Stone and H. Wyld, Nucl. Phys. **B275** (1986) 296; M.-P. Lombardo, J.B. Kogut and D.K. Sinclair, Phys. Rev. **D54** (1996) 2303.
143. I. M. Barbour, S. E. Morrison, E. G. Klepfish, J. B. Kogut and M.-P. Lombardo, *Results on Finite Density QCD*, hep-lat/9705042.
144. I.M. Barbour, S. Morrison and J. Kogut, *Lattice gauge theory simulation at nonzero chemical potential in the chiral limit*, hep-lat/9612012.
145. I. Barbour, A. Bell, M. Bernaschi, G. Salina and A. Vladikas, Nucl. Phys. **B386** (1992) 683.
146. M.A. Halasz, Nucl. Phys. **A642** (1998) 324.
147. J. Vink, Nucl. Phys. **B323** (1989) 399.
148. J. Kapusta, *Thermal Field Theory*, Cambridge University Press.
149. D. Bailey, *A Fortran-90 Based Multiprecision System*, NASA Ames RNR Technical Report RNR-94-013.

- 150. C.N. Yang and T.D. Lee, Phys. Rev. **87** (1952) 104, 410.
- 151. V. Matteev and R. Shrock, J. Phys. A: Math. Gen. **28** (1995) 5235.
- 152. D.A. Parshin and H.R. Schober, Phys. Rev. **B57** (1998) 10232.
- 153. Th. Schäfer, Phys. Rev. **D57** (1998) 3950.
- 154. C. Baillie, K. Bowler, P. Gibbs, I. Barbour and M. Rafique, Phys. Lett. **197B** (1987) 195.
- 155. M. Halasz, J. Osborn and J. Verbaarschot, Phys. Rev. **D56** (1997) 7059.
- 156. Y. Fyodorov and H. Sommers, JETP Lett. **63** (1996), 1026.
- 157. Y. Fyodorov, B. Khoruzhenko and H. Sommers, Phys. Lett. **A 226** (1997) 46.
- 158. K. Efetov, Phys. Rev. Lett. **79** (1997) 491; Phys. Rev. **B 56** (1997) 9630.
- 159. A.V. Kolesnikov and K.B. Efetov, cond-mat/9809173.
- 160. Y. Fyodorov, B. Khoruzhenko and H. Sommers, Phys. Rev. Lett. **79** (1997) 557.
- 161. K. Jansen, C. Liu, H. Simma and D. Smith, Nucl. Phys. Proc. Supp. **53**, 262 (1997).
- 162. G. Parisi, J. Phys. A: Math. Gen. **14** (1981) 735.
- 163. A.V. Andreev, O. Agam, B.D. Simons and B.L. Altshuler, Nucl. Phys. **B482** (1996) 536.
- 164. A. Altland and M. Zirnbauer, Phys. Rev. Lett. **77** (1996) 4536.
- 165. A.V. Andreev, B.D. Simons, and N. Taniguchi, Nucl. Phys **B432** [FS] (1994) 487.
- 166. M.R. Zirnbauer, chao-dyn/9810016.
- 167. M.R. Zirnbauer, chao-dyn/9812023.